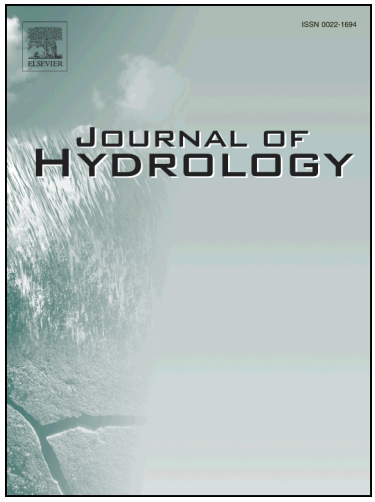


Research papers

# The challenges of modelling phosphorus in a headwater catchment: Applying a 'limits of acceptability' uncertainty framework to a water quality model

M.J. Hollaway, K.J. Beven, C.McW.H. Benskin, A.L. Collins, R. Evans, P.D. Falloon, K.J. Forber, K.M. Hiscock, R. Kahana, C.J.A. Macleod, M.C. Ockenden, M.L. Villamizar, C. Wearing, P.J.A. Withers, J.G. Zhou, N.J. Barber, P.M. Haygarth

PII: S0022-1694(18)30072-6
DOI: https://doi.org/10.1016/j.jhydrol.2018.01.063
Reference: HYDROL 22545

To appear in: *Journal of Hydrology*

Received Date: 26 May 2017
Revised Date: 21 December 2017
Accepted Date: 30 January 2018

Please cite this article as: Hollaway, M.J., Beven, K.J., Benskin, C.McW.H., Collins, A.L., Evans, R., Falloon, P.D., Forber, K.J., Hiscock, K.M., Kahana, R., Macleod, C.J.A., Ockenden, M.C., Villamizar, M.L., Wearing, C., Withers, P.J.A., Zhou, J.G., Barber, N.J., Haygarth, P.M., The challenges of modelling phosphorus in a headwater catchment: Applying a 'limits of acceptability' uncertainty framework to a water quality model, *Journal of Hydrology* (2018), doi: https://doi.org/10.1016/j.jhydrol.2018.01.063

# The challenges of modelling phosphorus in a headwater catchment: Applying a 'limits of acceptability' uncertainty framework to a water quality model

Hollaway, M.J.[1], Beven, K.J.[1],Benskin, C.McW.H.[1], Collins, A.L.[2], Evans, R.[3], Falloon, P.D.[4], Forber, K.J.[1], Hiscock, K.M.[5], Kahana, R.[4], Macleod, C.J.A.[6], Ockenden, M.C.[1], Villamizar, M.L.[7], Wearing, C.[1], Withers, P.J.A.[8], Zhou, J.G.[9], Barber, N.J.[10] Haygarth, P.M.[1]

[1] Lancaster Environment Centre, Lancaster University, Bailrigg, Lancaster LA1 4YQ, England, UK

[2] Rothamsted Research North Wyke, Okehampton, Devon EX20 2SB, England, UK

[3] Global Sustainability Institute, Anglia Ruskin University, Cambridge CB1 1PT, England, UK

[4] Met Office Hadley Centre, Exeter, Devon EX1 3PB, England, UK

[5] School of Environmental Sciences, Norwich Research Park, University of East Anglia, Norwich NR4 7TJ, England, UK

[6] James Hutton Institute, Aberdeen AB15 8QH, Scotland, UK

[7] School of Engineering, Liverpool University, L69 3GQ, England, UK

[8] School of Environment, Natural Resources and Geography, Bangor University, Bangor, Gwynedd LL57 2UW, Wales, UK

[9] School of Computing, Mathematics and Digital Technology, Manchester Metropolitan University, Manchester M1 5GD, England, UK

[10] Geography Department, Durham University, Durham, DH1 3LE, England, UK

Corresponding author: Michael Hollaway (m.hollaway@lancaster.ac.uk)

**Abstract**

There is a need to model and predict the transfer of phosphorus (P) from land to water, but this is challenging because of the large number of complex physical and biogeochemical processes involved. This study presents, for the first time, a 'limits of acceptability' approach of the Generalized Likelihood Uncertainty Estimation (GLUE) framework to the Soil and Water Assessment Tool (SWAT), in an application to a water quality problem in the Newby Beck Catchment (12.5km$^2$), Cumbria, United Kingdom (UK). Using high frequency outlet data (discharge and P), individual evaluation criteria (limits of acceptability) were assigned to observed discharge and P loads for all evaluation time steps, identifying where the model was performing well/poorly and to infer which processes required improvement in the model structure. Initial limits of acceptability were required to be relaxed by a substantial amount (by factors of between 5.3 and 6.72 on a normalized scale depending on the evaluation criteria used) in order to gain a set of behavioral simulations (1001 and 1016, respectively out of 5,000,000). Of the 39 model parameters tested, the representation of subsurface processes and associated parameters, were consistently shown as critical to the model not meeting the evaluation criteria, irrespective of the chosen evaluation metric. It is therefore concluded that SWAT is not an appropriate model to guide P management in this catchment. This approach highlights the importance of high frequency monitoring data for setting robust model evaluation criteria. It also raises the question as to whether it is possible to have sufficient input data available to drive such models so that we can have confidence in their predictions and their ability to inform catchment management strategies to tackle the problem of diffuse pollution from agriculture.

Keywords: SWAT, GLUE, phosphorus, uncertainty analysis, River Eden, high frequency data.

## 1 Introduction

In response to water quality targets set under the Water Framework Directive (WFD) (EC 2000/60/EC European Union 2000), it is imperative that we understand the sources, mobilization and delivery of diffuse pollution from agricultural land in headwater catchments to the river network (Haygarth et al., 2005; Perks et al., 2015). In order to devise management strategies that reduce the transfer of macronutrients (e.g. phosphorus (P) and nitrogen (N)) to river networks (McGonigle et al., 2014), models are essential tools in predicting how catchments may respond to key pressures in the present and into an uncertain future. Under climate change, winters are expected to become wetter and warmer, whilst summers are predicted to be hotter and drier in the United Kingdom (UK; Jones et al., 2010). Coupled with extended periods of drought, and an increase in extreme precipitation events for much of the UK (Kendon et al., 2014), these changes are likely to result in increased P transfers to waterways (Haygarth et al., 2005; Macleod et al., 2012; Ockenden et al., 2017).

Process based models are often used to assess the response of river systems to changes in land use and future climate drivers (Bosch et al., 2014; Crossman et al., 2013; Crossman et al., 2014; El-Khoury et al., 2015; Jin et al., 2015; Whitehead et al., 2013). These models are typically considered over-parameterized, with large numbers of interacting parameters governing the key physical and biogeochemical processes represented in the model structure (Beven, 2006; Dean et al., 2009; Krueger et al., 2007). While the parameters of such models may have some physical significance, 'effective' values of those parameters are required to account for variability in the catchment, key processes and the model limitations (Beven, 1996; Beven, 2002; Beven, 2006), with these frequently estimated through a combination of manual and automated calibration procedures.

Beven (2006) also highlighted that there is often limited information in the model calibration data to effectively identify calibrated values for model parameters. For example,

infrequent water quality data collection, which does not fully pick up catchment dynamics can lead to uncertainty in P load calculations (Johnes, 2007) which then impacts on the ability of the models to simulate catchment water quality accurately (Radcliffe et al., 2009). This uncertainty, coupled with other sources of uncertainty, results in equifinality, where multiple and very different parameter sets produce an equally acceptable fit to observations (Beven, 2006). A so-called 'optimum' parameter set will not then be robust to a change in the period of calibration data. In some cases, parts of a data set may not be informative in calibrating and evaluating a model (Beven and Smith, 2015). Furthermore, the concept of equifinality has been exhibited in the observed biogeochemistry of a catchment whereby signals in the observations can be explained by a large number of interacting processes (Haygarth et al., 2012).

Understanding how well these process-based models represent the key processes in the source, mobilization and delivery continuum, will improve their ability as learning tools in helping to unravel the complex interactions occurring in a catchment. This is particularly the case where the processes are often difficult or impossible to measure at the catchment scale (e.g. phosphorus concentrations in different nutrient pools in the soil). As a result, in recent years the impact of such uncertainties has received increased attention in water quality modelling (Dean et al., 2009; Harmel et al., 2014; Karamouz et al., 2015; Page et al., 2007; Vrugt and Sadegh, 2013; Woznicki and Nejadhashemi, 2014; Yen et al., 2015).

The Generalized Likelihood Uncertainty Estimation (GLUE) methodology (Beven and Binley, 1992) is an uncertainty estimation technique widely applied in the field of environmental modelling, including water quality models (Dean et al., 2009; Krueger et al., 2010; Krueger et al., 2009; Krueger et al., 2012; Page et al., 2003; Page et al., 2007; Page et al., 2004; Rankinen et al., 2006). GLUE evaluates model realizations for acceptability in the face of uncertainty in the model structure, parameters and input data. It accepts the

equifinality concept in using a set of acceptable or behavioral models to estimate the uncertainty in model predictions. It also provides a framework to evaluate a model as fit for purpose in representing the dynamics of a catchment using a set of evaluation criteria.

In this study, GLUE is used with a 'limits of acceptability' approach to evaluate a model parameter set, which should take into account the inherent error in the calibration data, such as errors in discharge data arising from rating curve uncertainties (Blazkova and Beven, 2009; Krueger et al., 2010; McMillan et al., 2012; McMillan and Westerberg, 2015; Pappenberger et al., 2006; Westerberg et al., 2011) and errors in water quality data (Krueger et al., 2012; Page et al., 2003; Page et al., 2004; Rankinen et al., 2006). The advantage of this approach is that it allows varying limits to be set for individual observations as well as combining evaluations based on different types of observations in a consistent way (Beven, 2006). Furthermore, it has been demonstrated that high frequency coupled hydrochemical data, allows short term changes in catchment dynamics to be better captured (Benettin et al., 2015; Halliday et al., 2015) and a greater understanding of the complex and non-linear interactions in the catchment system to be obtained. This is particularly the case in flashy catchments where storm events can lead to rapid changes in stream concentrations of P, and thus allows more robust and empirically defined model evaluation criteria to be set. However, the reality of not having such high quality data available can often make it difficult to define appropriate limits (Dean et al., 2009).

The Soil and Water Assessment Tool (SWAT; Arnold et al., 1998; Gassman et al., 2007) is one such process-based model that has been the focus of uncertainty and calibration procedures in recent years (Arnold et al., 2012; Karamouz et al., 2015; Schuol and Abbaspour, 2006; Shen et al., 2012a). Designed to simulate the impacts of management and mitigation on biogeochemistry and water quality in ungauged river basins, development of SWAT began in the early 1990s (Gassman et al., 2007). The model has been continually

improved over the years and has incorporated key components based on those in other established models. These include the hydrology component from the Chemicals, Runoff, and Erosion from Agricultural Management Systems (CREAMS) model (Knisel, 1980), the pesticide component from the Groundwater Loadings Effects on Agricultural Management Systems (GLEAMS) model (Leonard et al., 1987) and the crop growth component from the Environmental Impact Policy Climate model (Izaurralde et al., 2006), which was previously known as the Erosion Productivity Impact Calculator (EPIC) model (Williams, 1990). Finally, river routing and instream kinetic routines were incorporated based around the Routing Options to Outlet (ROTO; Arnold et al., 1995) and QUAL2E (Brown and Barnwell Jr., 1987) models respectively.

The GLUE framework has been applied to SWAT before (Karamouz et al., 2015; Shen et al., 2012a) with the Nash-Sutcliffe efficiency (NSE) typically used as the likelihood measure. A prescribed threshold is used to define behavioral simulations, with focus tending to be on how the model performs in the medium to long term (typically monthly to yearly). These studies demonstrated that high uncertainty exists in the model predictions with a number of key parameters for flow and nutrient processes being unidentifiable due to limitations in the model input and calibration data (Shen et al., 2012a). However, due to limited computational power, these studies sampled only a small area of the parameter space (10,000 iterations for a 20 parameter space) and hence could miss sampling potentially behavioral parameter sets. Further to this, previous uncertainty applications to SWAT focus largely on using summary statistics such as NSE to evaluate model performance (Shen et al., 2012a; Shen et al., 2012b; Shen et al., 2013) and do not focus on those time-steps critical to model failure. Finally, whilst there have been previous studies with SWAT that are concerned with the effects of input data uncertainty on model performance (Shen et al., 2012b; Shen et al., 2013), no previous study accounts for uncertainty in the data used to calibrate the model.

This work provides for the first time, a 'limits of acceptability' approach of the GLUE framework to the SWAT model in an application to the Newby Beck sub-catchment of the River Eden Basin in Cumbria, UK. This study takes advantage of the high temporal resolution water quality monitoring data set from the Demonstration Test Catchments (DTC) project (McGonigle et al., 2014) to gain a better understanding of the uncertainty in the predictions of models such as SWAT by using the 'limits of acceptability' to identify exact time-steps critical to model failure. This will provide an insight as to whether it is suitable to use SWAT as a catchment management tool in the Newby Beck sub-catchment. We do this by evaluating whether it can adequately represent the key dynamics of P transport to the stream, whilst also explicitly accounting for errors in calibration data. This study has the following objectives.

1) What are the critical time-steps causing the model to be classed as not acceptable?
2) What can be learned from the uncertainty in the model predictions to better understand the complex interactions occurring at the catchment scale?
3) Can we identify which processes require further investigation in the model structure and do we have sufficient input data to drive such complex models?

## 2 Materials and Methods

### 2.1 Catchment description and observations

Newby Beck (Figure 1) is a small headwater sub-catchment located in the River Eden basin in the North West of England, in the United Kingdom. The catchment is approximately 12.5 $km^2$ in size with an average elevation of 234 m above sea level (Owen et al., 2012; Perks et al., 2015). The underlying geology is dominated by Carboniferous limestone, which is overlain by low-permeability glacial deposits. There are well drained, fine and loamy soils

over limestone (Waltham soil association (541q)) in the upper reaches, seasonally wet deep loamy soils in drift from Paleozoic sandstone and shale in the mid-reaches (Brickfield 3 soil association (713g) and seasonally waterlogged reddish fine and coarse loamy soils in glacial till (Clifton soil association (711n) in the lower reaches of the catchment (National Soil Resources Institute (NSRI) Cranfield University 2014). The dominant soil unit in the catchment is the 713g Brickfield association, which covers approximately 66% of the basin area. The primary land use in the catchment is improved grassland (approximately 76% by area) which is used for a mix of dairy and beef production. Other land uses are rough grassland (14%), arable (6%), woodland (2.5%) and built-over land (0.5%; Morton et al., 2011). The climate of the region is cool temperate maritime with an annual average rainfall of around 1200 mm. Due to the underlying geology, the 23% of the catchment area is greater than 5°, which results in rapid catchment response time leading to a time-to-peak of about 3 hours (Perks et al., 2015). Based on the Hydrology of Soil Types (HOST) classifications, the catchment has a standard percent runoff of 35% (Perks et al., 2015), resulting in very flashy responses of the hydrograph to rainfall events and high occurrences of saturated overland flow (Ockenden et al., 2016).

**Figure 1: Summary of spatial data in the Newby Beck catchment. Panel a) shows the catchment topography, panel b) shows the locations of the monitoring station (discharge and total phosphorus (TP)), weather station and rain gauges, panel c) shows the main soil classes in the catchment and panel d) shows the broad land use classifications.**

The catchment outlet was a rated section of channel used to provide high frequency discharge data at 15-minute intervals. The discharge measurements were calculated from a time series of stage measurements (obtained with a SWS mini-Diver) using site-specific

rating curves. In addition, a high frequency bankside monitoring station was situated at the outlet, which recorded nitrate ($NO_3$), total P (TP) and total reactive P (TRP) at 30 minute intervals (Outram et al., 2014). The TP and TRP measurements were conducted using a Hach Lange combined Sigmatax sampling module and Phosphax Sigma analyzer (Perks et al., 2015). Rainfall was recorded at 15-minute intervals by three tipping bucket rain gauges. Other meteorological data was provided by an Automatic Weather Station (AWS), which was located towards the centre of the catchment (Figure 1). Daily rainfall data was also gained from a rain gauge located in the center of Newby Beck catchment from the Met Office Integrated Data Archive System (MIDAS) network (Met Office 2012). The location of the monitoring stations, rain gauges, and outlet monitoring station are shown in Figure 1. Information on fertilizer and manure applications were based around a typical dairy and beef grassland catchment system with guidance from the Defra fertilizer handbook (Rb209; Defra, 2013) and available farm diary data for the catchment for the years 2011-2014.

## 2.2 Implementation of the SWAT model to Newby Beck

The SWAT model (version 2012, revision 637) is a semi-distributed, process-based model (Arnold et al., 1998; Gassman et al., 2007) which simulates surface and sub-surface hydrology, along with various nutrient (including P) and sediment fluxes, at a basin scale. The model also incorporates various land management practices along with a crop growth model in order to simulate the impact of agriculture at the catchment scale. SWAT also includes urban area management practices and can incorporate pollution from point sources such as sewage treatment works. The model requires spatial information including land use, soil type and elevation, which are often input as GIS layers. Additional inputs required include any land management practices (e.g. fertilizer application rates and animal stocking densities) and weather data including rainfall, temperature, wind speed, humidity and solar

radiation. In order to reduce the computational complexity of SWAT, a semi-distributed approach is taken such that the model lumps unique land, soil and slope combinations into hydrological response units (HRUs) within each sub-basin of the main catchment. The hydrological and biogeochemical model processes are calculated for each HRU and then lumped to produce a response for each sub-basin.

To implement SWAT for the Newby Beck catchment, the NextMap 5m digital elevation model (DEM) dataset (Intermap Technologies 2009) was used to delineate the catchment boundary highlighted in Figure 1. Land use (25 m resolution) was from the Centre of Ecology and Hydrology (CEH) land cover map (LCM) 2007 (Morton et al., 2011), which indicates the most likely Broad Habitat land classification for each 25m grid square. Soil properties (1 km resolution) were determined from the NSRI database (Cranfield University2014). In order to keep the simulation as computationally efficient as possible, the catchment was divided spatially into 3 sub-basins, each with a different mean elevation. Within each sub-basin, HRUs were defined based upon the unique combinations of the LCM land cover class (the dominant proportion of coverage in each grid square) and the dominant soil association (Brickfield (713g), resulting in 5 HRUs per sub-basin and 15 in total (Figure 1). Fertilizer application rates for each land class were lumped up to HRU level to provide an average nutrient application rate for each response unit. Finally, the required precipitation and weather data were provided by the rain gauges and the AWS (Figure 1).

SWAT was set up to produce daily predictions of discharge and TP loads. A sub-daily variant of the model was available (Gassman et al., 2007), however, at present it does not produce sub-daily output for nutrients. Therefore in this study we have used the daily time-step variant of the model which has been used in numerous previous studies (Shen et al., 2012a; Shen et al., 2013; Taylor et al., 2016; Wang and Sun, 2016; Zhang et al., 2014). Model simulations are evaluated using daily observations of discharge and TP loads, which

are calculated from the high frequency data at the catchment outlet. The modified SCS curve number method was used for computing surface runoff volume. While often used as a representation of infiltration excess runoff, Steenhuis et al. (1995) have shown that it can also be interpreted in terms of saturation excess contributing areas which is more appropriate for the study catchment. The Penman Monteith (Monteith, 1965) method was used to calculate evapotranspiration and the Muskingham routing method (Brakensiek, 1967; Overton, 1966) to route water in the river network. P is cycled through the soil through a combination of leaching, mineralization, decomposition and immobilization processes and surface runoff is largely assumed to be the primary transport route into the river network (Neitsch et al., 2011). The algorithms for each respective process are solved and P is moved between respective soil stores and into the river network to ensure that mass balance is conserved.

The model was run with a two year warm up period and was calibrated over the 2011-2012 and 2012-2013 hydrological years and validated over the 2013-2014 hydrological year.

2.3 The limits of acceptability GLUE uncertainty framework

The performance of the SWAT simulations was assessed using the GLUE methodology (Beven and Binley, 1992; Beven and Binley, 2014). GLUE was extended to use the limits of acceptability approach described by Beven (2006; 2009) and applied in previous applications to hydrological (Blazkova and Beven, 2009; Krueger et al., 2010; Liu et al., 2009) and water quality models (Krueger et al., 2012; Page et al., 2003; Page et al., 2004; Rankinen et al., 2006).

GLUE recognizes that for any given observational data set and performance criteria there may be multiple model parameter sets and structures that produce acceptable simulations. Each application is dependent on a number of decisions:

1. Choose which model parameters to vary

2. Choose which model structures to consider (e.g. whether in stream processing of nutrients is switched on or off)
3. Define prior distributions within which to sample each parameter
4. Determine the limits of acceptability used to assess the performance of a model run
5. Decide on a likelihood measure for creating the uncertainty prediction bounds given a set of behavioral models

In the absence of any knowledge regarding the prior probability distributions of effective parameter values, random uniform sampling was utilized between defined prior ranges. However, if this information is known it can be incorporated into the sampling strategy.

To assess if a given parameter set is behavioral, limits of acceptability are specified for each observation at each time-step during the calibration period, to take into account the inherent uncertainty in the calibration data. Model performance (*Score(t)*) is determined at each time-step, *t,* by how well the simulated value satisfies these limits and are normalized as follows to compare limits over different measures,

$$\text{Score}(t) = \begin{cases} (\hat{Y}_t - y_t)/(y_t - y_{min,t}) & \hat{Y}_t < y_t \\ (\hat{Y}_t - y_t)/(y_{max.t} - y_t) & \hat{Y}_t \geq y_t \end{cases} \quad (1)$$

where $\hat{Y}_t$ is the simulated value; $y_t$ is the best estimate of the observed value; $y_{min,t}$ is the lower limit of acceptability; and $y_{max,t}$ is the upper limit of acceptability for a given time-step. This results in scores that are zero at the best estimate of an observed value, -1 at the lower limit and +1 at the upper limit. For a model to be considered behavioral, all scores must fall within the limits at every time step (between -1 and +1).

The first step in defining the limits of acceptability is to consider the range of output observational uncertainty. For discharges, this will depend on both water level measurement uncertainty and rating curve uncertainties (e.g. McMillan and Westerberg (2015)). For water quality load variables, it will depend on uncertainties in discharge, sampling and measurement of determinand concentrations in addition to their aggregation to the temporal and spatial scales of interest (McMillan et al., 2012). Where such uncertainties are estimated using fuzzy or interval arithmetic, then limits of acceptability can be defined directly (Krueger et al., 2010; Krueger et al., 2009; Krueger et al., 2012; Pappenberger et al., 2006; Westerberg et al., 2011). However, where such uncertainties are estimated statistically, there are normally no sharp limits on the potential ranges (the assumed distributions will have infinite tails). In this case, it is necessary to truncate the uncertainty (normally at the 95% or 99% level).

Where such limits of acceptability are based only on the output observational uncertainties, they provide a minimal range of acceptable behavior because no explicit account has been taken of the effect of input uncertainty. This is more difficult to do since the nonlinear dynamics of most models make it difficult to assess the impact of input error independently of the model. There is, however, the option of exploring input error propagation within the GLUE framework (Krueger et al., 2010; Krueger et al., 2009; Krueger et al., 2012; Page et al., 2003; Page et al., 2004). In this paper, an indirect approach was taken by relaxing the limits until a given number of behavioral simulations have been accepted. We discuss a number of ways of doing so. It can be done by imposing the condition that only a certain percentage of the scores must fall within the -1 to +1 scores (e.g. 95%/99%) or by finding the minimum extension required of the limits for simulations to be considered behavioral. This degree of relaxation can then be used to determine, at least subjectively, whether the model can be considered as fit-for-purpose.

Once a set of behavioural simulations have been identified a final likelihood weight needs to be calculated for each behavioural model. First, a weight *W* is calculated at each evaluation time-step *t* using Equation 2.

$$W(t)\begin{cases}[(Score(t)-L_{lwr})/abs(L_{lwr})]^N & L_{lwr} \le Score(t) < 0 \\ \left[\left(L_{upr}-Score(t)\right)/abs\left(L_{upr}\right)\right]^N & 0 \le Scores(t) < L_{upr} \\ 0 & Score(t) \notin \left(L_{lwr}, L_{upr}\right)\end{cases} \quad (2)$$

where *Score(t)* is the normalized score at time-step *t*, and $L_{lwr}$ and $L_{upr}$ are the lower and upper criteria to consider the set of models behavioural for the required number of time steps. *N* is a shaping factor, which is set at 1 in this case, following the approach of Liu et al. (2009). This is a similar approach to applying a triangular fuzzy weight at each evaluation time-step (Freer et al., 2004; Liu et al., 2009).

The weights at each time-step are then combined to produce an overall likelihood weighting for each behavioural model:

$$L\left(M(\theta_i|Y)\right) \propto \sum_{t=1}^{T} W(t) \quad (3)$$

where *T* is the total number of time steps and *W(t)* is a triangular fuzzy weighting at time-step *t*. As previously in GLUE, prediction quantiles can then be formulated at any given time-step (*t*) by calculating the likelihood weighted cumulative density function of a predicted variable over the set of behavioural models.

$$P\left(\hat{Z}_t < z_t\right) = \sum_{j=1}^{j=N} L\left[M\left(\Theta_j\right)|\hat{Z}_{t.j} < z_t\right] \quad (4)$$

where $P$ is the prediction quantile for $\hat{Z}_t$ (the simulated value of variable $Z$ at time step $t$ using model $M(\Theta_j)$) being less than $z$; $L$ is the likelihood weighting associated with model $M(\Theta_j)$; $\Theta_j$ is the $j$th parameter set; and $N$ is the number of models accepted as behavioral.

In this study, the model was evaluated using daily discharge and TP loads with the constraint imposed that for both discharge and TP loads the simulated value must fall within the limits of acceptability at all time-steps throughout the calibration period (2011-2012 and 2012-2013 hydrological years). This period totaled 731 time-steps and accounting for both upper and lower limits gave 1462 limits to satisfy for discharge. For TP loads, there were 1210 limits to satisfy, due to missing data, giving a total of 2672 limits to be met for a model run to be considered behavioural. This allows likelihood measures to be calculated for discharge ($L_Q$) and TP ($L_{TP}$), respectively. For each behavioral model run, an overall likelihood ($L_{ovr}$) can be constructed as follows

$$L_{ovr} = \frac{L_Q \cdot L_{TP}}{C} \tag{5}$$

where $C$ is a scaling factor such that the sum of likelihoods scales to unity in each case. Equation 4 can then be applied to determine the uncertainty bounds on the model predictions.

Here, thirty two parameters in the SWAT model considered important for hydrology and water quality processes (Arnold et al., 1998; Gassman et al., 2007; van Griensven et al., 2006) were sampled uniformly between the ranges detailed in the model user manual (Table 1). As some parameters varied with land use, a total of 39 were included in the Monte-Carlo simulations. In order to preserve the spatial heterogeneity of the soil and curve number parameters across HRUs, multipliers were applied during the Monte Carlo simulations (Table 1). The ranges and parameters chosen in Table 1 were based around an initial sensitivity

analysis. For such a large parameter space, many model runs were required and SWAT was implemented on the Lancaster University HEC (High End Computing) facility. The results presented are based on 5,000,000 iterations of the SWAT model executable (version 2012, revision 637), run within an R wrapper (R Core Team, 2016) which sampled the parameters uniformly between the ranges specified in Table 1.

**Table 1: SWAT model parameters and ranges used within the Generalized Likelihood Uncertainty Estimation (GLUE) framework. The values of each parameter were sampled on a random uniform basis between the ranges.**

| Parameter | Description | Min Value | Max Value |
|---|---|---|---|
| **CN2*** | SCS runoff curve number | -0.2 | 0.2 |
| **USLE_P_FRSD** | USLE[a] equation support practice factor (forest) | 0.0 | 0.5 |
| **USLE_P_AGRL** | USLE[a] equation support practice factor (arable) | 0.0 | 1.0 |
| **USLE_P_PAST** | USLE[a] equation support practice factor (pasture) | 0.0 | 0.5 |
| **USLE_P_RGRS** | USLE[a] equation support practice factor (rough grazing) | 0.0 | 1.0 |
| **USLE_P_URML** | USLE[a] equation support practice factor (urban) | 0.0 | 1.0 |
| **ALPHA_BF** | Baseflow alpha factor (1/days) | 0.0 | 1.0 |
| **GW_DELAY** | Groundwater delay (days) | 26.0 | 500.0 |
| **GWQMN** | Threshold in shallow aquifer for return flow (mm) | 970.0 | 3300.0 |
| **RCHRG_DP** | Deep aquifer percolation fraction | 0.4 | 1.0 |
| **LAT_ORGP** | Organic P in baseflow ($mgl^{-1}$) | 0.0 | 0.1 |
| **GWSOLP** | Concentration of soluble P in groundwater flow($mgl^{-1}$) | 0.0 | 0.1 |
| **GW_REVAP** | Groundwater "revap" coefficient | 0.02 | 0.2 |
| **REVAPMN** | Threshold depth in shallow aquifer for "revap" to occur (mm) | 150.0 | 500.0 |
| **SLSOIL** | Slope length for lateral subsurface flow (m) | 10.0 | 45.0 |
| **CANMX_FRSD** | Maximum canopy storage for forest ($mmH_2O$) | 0.0 | 100.0 |
| **CANMX_AGRL** | Maximum canopy storage for arable ($mmH_2O$) | 0.0 | 100.0 |
| **CANMX_PAST** | Maximum canopy storage for pasture ($mmH_2O$) | 0.0 | 100.0 |
| **CANMX_RGRS** | Maximum canopy storage for rough grazing ($mmH_2O$) | 0.0 | 100.0 |
| **LAT_TTIME** | Lateral flow travel time (days) | 0.0 | 1.8 |
| **ERORGP** | Phosphorus enrichment ratio for loading with sediment | 0.0 | 5.0 |
| **CH_N2** | Manning's "n" value for the main channel | 0.0 | 0.3 |
| **CH_COV1** | Channel erodibility factor | 0.0 | 1.0 |
| **CH_COV2** | Channel cover factor | 0.0 | 1.0 |
| **SOL_K*** | Saturated hydraulic conductivity (mm/hr) | 0.0 | 2.0 |
| **USLE_K*** | USLE[a] equation soil erodibility factor (ton $m^2$ hr/$m^3$-ton cm) | -0.1 | 0.1 |
| **SOL_ORGP** | Initial organic P concentration in soil layer ($mgl^{-1}$) | 0.1 | 100.0 |
| **SOL_LABP** | Initial labile P concentration in soil layer ($mgl^{-1}$) | 0.1 | 100.0 |
| **CH_N1** | Manning's "n" value for tributary channels | 0.06 | 0.15 |
| **SURLAG** | Surface runoff lag coefficient | 2.0 | 24.0 |
| **ESCO** | Soil evaporation compensation factor | 0.4 | 0.9 |
| **EPCO** | Plant uptake compensation factor | 0.1 | 0.9 |
| **SPEXP** | Parameter for amount of sediment reentrained in routing | 1.0 | 1.5 |
| **SPCON** | Parameter for amount of sediment reentrained in routing | 0.001 | 0.01 |

| | | | |
|---|---|---|---|
| **PSP** | P sorption coefficient | 0.01 | 0.7 |
| **CMN** | Rate factor for mineralization of organic N | 0.001 | 0.003 |
| **RSDCO** | Residue decomposition coefficient | 0.02 | 0.1 |
| **PPERCO** | P percolation coefficient (global) | 10.0 | 17.5 |
| **P_UPDIS** | P uptake distribution parameter | 10.0 | 100.0 |

*These parameters were varied relatively using a random multiplier between the ranges in order to preserve the spatial heterogeneity of the parameters.
[a]USLE= Universal Soil Loss Equation.

2.4 Sources of uncertainty in the calibration data

In order to set initial limits of acceptability for discharge and TP loads, the uncertainty in the rating curve and in-situ TP concentration measurements were first examined. The methodology of deriving these limits is described briefly below with more detail available in Hollaway et al (In Prep). To produce a rating curve the Velocity Area Rating Extension (VARE) model was used (Ewen et al., 2010), which uses the water balance and an assumed maximum river velocity to constrain the extrapolation of the curve beyond the gauged range. An extended version of the voting point likelihood methodology (McMillan and Westerberg, 2015) was used in a Monte Carlo Framework to calibrate the rating curve. In brief, the voting point method works by evaluating candidate rating curves (from the Monte Carlo sampling) against the observations (and in the VARE method constrained by the water balance). A candidate curve is considered behavioural if it falls within the uncertainty bounds of at least one of the observations and is weighted based upon A) the number of measurements it intersects and B) how close it lies to the true value (in this case we use a triangular weighting). Finally, 95% confidence limits are derived from all behavioural curves and their associated weightings to give the uncertainty limits on the discharge time series.

The resultant uncertainty (based on 95% prediction quantiles) on discharge was on average 96% with a range of 24-163%. This range is much larger compared to those determined during a recent study on 500 UK catchments (Coxon et al., 2015), which showed that the majority of catchments had 20-40% relative uncertainty intervals, though the maximum

uncertainty of 163% determined for Newby Beck here is much lower than the maximum value of 397% quoted by Coxon et al. (2015).

As daily TP loads are determined from both discharge and in stream TP concentrations. To evaluate the uncertainty on the in-situ concentrations, measurements from the bankside analyser were paired with land analysed grab samples and ISCO data. An empirical power law was then fitted, once again using a voting point likelihood in a Monte-Carlo framework. In this case, the lab-analysed sample was assumed representative of the true concentration. Finally, the unique combination of behavioural parameter sets from both the discharge and TP time series were used to estimate the uncertainty on the resultant TP load.

For the in-situ TP concentrations from the bankside analyser, uncertainty intervals ranged from 231% for the lower concentrations (the bottom 5%) to around 81% for the highest concentrations. When combined with the discharge uncertainty this resulted in an average 271% for the lowest loads (bottom 5%) and 76% for the highest loads.

## 3 Results

### 3.1 Model performance and rejection

For the initial limits of acceptability (see 2.4), none of the 5,000,000 parameter sets sampled produced a model that satisfied the limits at every time-step for both discharge and TP loads. In order to investigate why the sampled parameter sets were not producing behavioural models a subset of the best parameter sets was chosen on which to perform further analysis. In order to identify this subset of models we took two different approaches. These two different methods were adopted to evaluate the sensitivity of accepted model parameter sets to the choice of evaluation measure. The first approach was to find the minimum relaxation of the normalized limits across all time-steps that was required to accept a set of 1000 models. The second approach was to only require the model to fall within the limits in the high and low flow time-steps. In this case, the thresholds for high and low flows

(for both discharge and TP) were set as the top and bottom 5% of discharges as defined from the flow duration curve. For this second evaluation measure if no parameter sets satisfied the initial limits of acceptability for all the selected time steps, they were again relaxed until a set of 1000 models was accepted on which to perform further diagnostics.

3.1.1 Evaluation across all model time-steps

When the normalized scores of acceptance were allowed to relax (based on normalized scores falling within the limits at all time-steps) to $\pm$ 6.72, 1016 simulations can be considered acceptable. In order to gain a better understanding of why such large relaxation of the limits was required, a more detailed examination of the scores was made for the accepted simulations to look for systematic deviations between the simulations and observations. Figure 2 shows a summary of the performance of the 1016 simulations against observations over all time-steps, for the rising/falling limbs of the hydrograph and for the high and low flow periods (as defined above). Figure 2 also shows a comparison of the normalized scores against the observations.

**Figure 2: Generalised likelihood uncertainty estimation (GLUE) likelihood distributions, based upon the evaluation of models using criteria set for all time steps (normalized scores of ± 6.72), of Qsim (simulated discharge), normalised score for Q (discharge), TP loadsim (simulated total phosphorus) and normalised scores for TP, respectively, against observations (panels A-D). The plots are repeated for the low flow periods (panels E-H), rising time-steps (panels I-L), falling (recession) time-steps (panels M-P) and high flow periods (panels Q-T). The areas between the distribution percentiles max/min, $5^{th}$/$95^{th}$ and $25^{th}$/$75^{th}$ are shown in grey shades of increasing intensity. The medians of the distribution are shown by black dots. 1:1 lines and normalised scores of 0 lines have been added for orientation.**

For both discharge (Figure 2E) and TP loads (Figure 2G) the models tend to show a bias towards over-prediction during the low flow periods. In contrast there is systematic under-prediction shown for both discharge (Figure 2Q) and TP (Figure 2S) during the high flow periods although the normalized scores show a tendency to be smaller for these periods which

reflects the larger absolute uncertainty intervals on the higher flow observations for both measures (Figure 2). Overall, the majority of scores which tend to be outside the original limits occur during the falling limb of the time-series, particularly for the lower magnitude flows and loads during these periods, which could be a constraint on model performance.

This under-prediction of peaks during the high flow periods is reflected in Figure 3, which shows the time series of the performance of the 1016 accepted models during the summer, autumn and early winter of the 2012-2013 hydrological year. Overall, the model captures the timings of the peaks and low flow periods fairly well, however the under-prediction of the peaks in December and January is emphasized for both discharge (Figure 3a) and TP loads (Figure 3b). Despite relatively high normalized scores shown in Figure 2 during the low flow periods, the over-prediction of observations is less emphasized in Figure 3 due to the smaller absolute widths of the uncertainty intervals at these time-steps. However, over-prediction is evident during the low flow period in late January 2013, particularly in the discharge time-series.

3.1.2. Evaluation across high and low flow periods only

When the model evaluation is constrained to the high and low time-steps (top and bottom 5% of time-steps across the flow duration curve), none of the 5,000,000 model runs fall within the original limits of acceptability. Hence, in order to gain a subset of model runs for the calculation of model diagnostics, we relaxed the limits to 5.30 to gain a set of 1001 behavioural simulations. Figure 4 shows a comparison of the model performance versus the observations over all time-steps, rising/falling time-steps and high/low flow time-steps. Overall, the picture is consistent when the models were constrained over all time-steps (section 3.2.1) with over-prediction of both discharge and TP during the low flow periods (Figure 4F and 4H) and under-prediction during the high flow periods (Figure 4R and 4T). However, much higher over-predictions are shown for lower discharge and TP loads,

particularly those classified as falling time-steps (Figure 4N and 4P respectively) where normalized scores approach 15 for discharge and 30 for TP. These higher scores (compared to Figure 2) reflect the fact that we are only constraining the model on a smaller number of time-steps, albeit these are the high and low flow periods that are often considered important to simulate accurately to best capture catchment dynamics. This once again shows that poor performance during the recession periods is a constraint on finding behavioural parameter sets for SWAT in application to this catchment.

**Figure 3: Generalized Likelihood Uncertainty Estimation (GLUE) weighted prediction bounds (green shading) for discharge (a) and total phosphorus loads (b) for Newby Beck outlet (part of the calibration period) based on normalized scores on both discharge and total phosphorus (TP) load evaluation measures when criteria (normalized scores of ± 6.72) set over all model time-steps (1016 simulations). The black line in each plot shows the observed discharge (a) and TP loads (b), respectively. The dashed lines show the uncertainty limits on the calibration data.**

**Figure 4: Generalised Likelihood Uncertainty Estimation (GLUE) likelihood distributions of, based upon the evaluation of models using criteria set for high and low flow periods only (normalized scores of ± 5.30), Qsim (simulated discharge), normalised score for Q (discharge), TP loadsim (simulated total phosphorus) and normalised scores for TP, respectively, against observations (panels A-D). The plots are repeated for the low flow periods (panels E-H), rising time-steps (panels I-L), falling (recession) time-steps (panels M-P) and high flow periods (panels Q-T). The areas between the distribution percentiles max/min, $5^{th}$/$95^{th}$ and $25^{th}$/$75^{th}$ are shown in grey shades of increasing intensity. The medians of the distribution are shown by black dots. 1:1 lines and normalised scores of 0 lines have been added for orientation.**

Figure 5 shows the time-series of model performance of the 1001 accepted models during the summer, autumn and early winter of the 2012-2013 hydrological year. In this case as the high and low flow periods that are being used to constrain the model the dynamics of the catchment are captured much better by the accepted simulations with the model capturing both the timing and magnitude of the peaks for both discharge (Figure 5a) and TP loads (Figure 5b). However, there is still under-prediction of peaks during December and early

January and over-prediction of low flow periods during late January with this once again most evident in the discharge time-series (Figure 5a).

**Figure 5: Generalized Likelihood Uncertainty Estimation (GLUE) weighted prediction bounds (green shading) for discharge (a) and total phosphorus loads (b) for Newby Beck outlet (part of the calibration period) based on normalized scores on both discharge and total phosphorus (TP) load evaluation measures when criteria (normalized scores of ± 5.30) set over high and low flow time-steps only (1001 simulations). The black line in each plot shows the observed discharge (a) and TP loads (b), respectively. The dashed lines show the uncertainty limits on the calibration data.**

3.2 Evaluation of model parameter uncertainty

Figure 6 shows projections of the sampled points on the likelihood surface (as calculated by Equation 5) onto single parameter axes for the parameters in Table 1 for each of the behavioral simulations. These have previously been called dotty plots and can be used to infer sensitivities of the individual parameters using the Hornberger-Spear-Young method (see Beven, 2009). The points shown are the 1016 simulations which satisfy the relaxed limits of acceptability for both discharge and P when evaluated across all time-steps. The same plot is shown in Figure 7 when the models are evaluated across the high and low flow period only. Both Figures 7 and 8 show consistency in the sensitivity of the parameters varied. Of the 39 parameters varied, only four parameters exhibited any clear identifiability. These are GW_DELAY (ground water delay), RCHRG_DP (deep aquifer percolation fraction), LAT_TTIME (lateral flow travel time) and LAT_ORGP (organic P in the baseflow). Further to this, behavioural models are identified at both high and low values of the GW_DELAY parameter, which is consistent across both evaluation metrics. Some levels of identifiability were shown for the CN2 (SCS runoff curve number) and SLSOIL (slope length for lateral subsurface flow), however the responses of these parameters differed between the method chosen to evaluate the models. For SLSOIL, when the model was evaluated on all time-steps, higher likelihood values were shown towards the higher end of

the sample range. The opposite was shown for evaluation over the high and low time-steps only with higher likelihood values shown towards the lower end of the sampled parameter range. Overall the majority of parameters showed no sign of sensitivity and indicated high equifinality across the sampled ranges.

**Figure 6: Dotty plots for 39 of the parameters varied in the Monte-Carlo runs. Parameter names and definitions are shown in Table 1. These are based on the 1016 behavioral simulations evaluated across all time-steps (normalized scores of ± 6.72).**

**Figure 7: Dotty plots for 39 of the parameters varied in the Monte-Carlo runs. Parameter names and definitions are shown in Table 1. These are based on the 1001 behavioral simulations evaluated across the high and low flow time-steps only (normalized scores of ± 5.30).**

The parameters that exhibit sensitivity are all linked to runoff and sub-surface processes and all interact to affect the time taken for water to reach the river network, and thus affect the transport of P. However, the high equifinality in the other parameters (particularly those in relation to the levels of P in the soils SOL_ORGP and SOL_LABP) indicates that given the present assumptions and data available for the catchment, there is not enough information to calibrate these parameters effectively.

3.3 Critical time-steps for model failure

Figure 8 shows a breakdown of the classification (high/low or rising/falling) of the time-steps of the sub-sample of models chosen on which to perform model diagnostics that result in model failure (lie outside the original limits of acceptability). For both evaluation measures used in this study, the falling limb time-steps contribute the largest proportion of failing time-steps for both simulated discharge (37% for all time-steps evaluation and 34% for evaluation on high/low time-steps) and TP loads (30% and 50% respectively). All other time step classifications contribute roughly the same to model failure with the rising limb and high

flow time-steps accounting for approximately 10-15% of failures for both discharge and TP. For discharge, the low flow time-steps account for around 10% of failures. However, for TP loads they provide a much smaller contribution at around 3-4% indicating that model performance at these time-steps may be less of a constraint on model performance for TP. Overall it is shown that despite using two different model evaluation measures to accept behavioural models, the falling limb time-steps are consistently shown to be a constraint on model performance in this SWAT application to Newby Beck.

3.4 Model validation.

The 1016/1001 behavioral simulations (all time steps evaluation/high and low flows evaluation) were then used to predict the discharge and P loads for a period not used in calibration (winter of the 2013-2014 hydrological year due to data availability) in order to validate the model performance (Figures 9 and 10). For discharge (Figures 9a and 10a), the picture was somewhat similar during the validation period where the model tended to pick out the timings of the peaks and recession periods well. Overall, under-prediction of the observed discharge peaks was seen throughout the validation period being most evident during mid-December 2013 and early January 2014. As when calibrating the model, the under prediction of peaks was more pronounced when the models were evaluated across all time-steps (Figure 9a). Both the timing and magnitude of the peaks was picked up much better when constraining the models on the high and low flow periods (Figure 10a). As in calibrating the model, the low flow periods were typically over-predicted by the model (on both evaluation measures) with this being most evident towards the end of January 2014.

**Figure 8: Breakdown of classification of time-steps resulting in model failure for the 1016 simulations constrained on all time-steps (upper panel) and the 1001 simulations constrained on the high and low flow periods only (lower panel). The bars show the median % contribution to failing time-steps and the error bars show the 2.5/97.5$^{th}$ percentiles from the Generalised likelihood uncertainty estimation (GLUE) weighted distributions.**

For TP loads, the picture is the same as during calibration with the model under-predicting all peaks, particularly when they were constrained using all time-steps where the model failed to capture the magnitude of any peak (Figures 9b and 10b). When constrained on the high and low flows time-steps only, the model reproduced the magnitudes and timings of the majority of the peak loads, however there are still cases where the model under predicts a peak by up to 75% (15$^{th}$ December 2013). Further to this the uncertainty bounds on the model predictions are much wider during the recession limbs of the TP time series, and shows over-prediction of the observations during this period.

**Figure 9: Generalized Likelihood Uncertainty Estimation (GLUE) weighted prediction bounds (green shading) for discharge (a) and total phosphorus (TP) loads (b) for Newby Beck outlet during the validation period (winter of the 2013-2014 Hydrological year) using the 1016 behavioral simulations accepted on both discharge and total phosphorus load criteria when evaluating constrained across all time-steps. The black line in each plot shows the observed discharge (a) and TP loads (b), respectively. The dashed lines show the uncertainty limits on the calibration data.**

## 4 Discussion

This work, presents for the first time, a 'limits of acceptability' GLUE uncertainty analysis of the widely used SWAT model, using continuous high frequency water quality measurements. It was shown that when initial limits of acceptability (based upon the uncertainty in the outlet data for the calibration period), are accounted for and given the assumptions detailed, none of the 5,000,000 simulations provided suitable predictability of the dynamics of the catchment (i.e. none of them were classed as behavioral).

**Figure 10: Generalized Likelihood Uncertainty Estimation (GLUE) weighted prediction bounds (green shading) for discharge (a) and total phosphorus (TP) loads (b) for Newby Beck outlet during the validation period (winter of the 2013-2014 Hydrological year) using the 1001 behavioral simulations accepted on both discharge and total phosphorus load criteria when evaluating constrained across high and low flow time-steps only. The black line in each plot shows the observed discharge (a) and TP loads (b), respectively.**

Therefore, in order to obtain behavioral simulations to investigate the uncertainty in the SWAT model predictions, a subset of samples was obtained on which to perform further diagnostics, with this subset chosen using two different criteria. The first was to find the minimum level of relaxation across all model time-steps in the calibration period required to consider the models acceptable. In this case relaxation of the limits to ±6.72 gave a subset of 1016 acceptable models. In the second case, we only required the models to fall within the relaxed limits during periods of high and low flow (here defined as the top and bottom 5% of discharges based on the flow duration curve). For these criteria, the limits had to be relaxed (over the high and low flow periods only) ±5.30 to give a subset of 1001 accepted models. This was across both discharge and TP loads.

Using these two different evaluation measures produced two distinctly different time series when the models were compared with observations (Figures 5 and 7) and during the validation period (Figures 9 and 10). When the models were constrained to fit within the limits across all time-steps the parameter sets that are considered acceptable consistently under predict the peaks in both discharge and TP loads, particularly during the validation period. In contrast, when we only constrain the model on the low and high flow periods, the simulations from the accepted parameter sets produce a much better representation of the catchment dynamics, particularly in the magnitudes of the TP load peaks. However, constraining the model in this way accepts simulations that have poor performance during the rising limb and recession periods where the normalized scores approach 15 in the case of discharge and 30 in the case of TP loads. This contrast between the chosen metric to evaluate the model is the result of several different factors and depends on the characteristics and dynamics of the Newby Beck catchment. Due to its flashy nature and low baseflow index (Ockenden et al., 2016; Outram et al., 2014), Newby Beck is dominated by sub-daily processes which may lead to timing errors in the simulated hydrograph from SWAT due to

the use of the daily time-step of the model. Therefore, when all time-steps are included in the evaluation metric, there is a high chance of the model simulations producing high normalized scores. However, as reported recently by (Coxon et al., 2014), constraining the model using time-step measures such as these can be a very critical test of the model, particularly due to the strong influence of observational uncertainty on such metrics (see Section 3.1). This is shown in Figure 3 where all of the accepted 1016 simulations (when using the all-time-step metric) under-predicted the peaks by a large amount for both discharge and TP loads, despite being considered acceptable within the relaxed limits of 6.72. This could be because the normalized scores are based upon the relative uncertainty intervals around the observations, which allows a larger absolute deviation from the observed value on the peaks. This is a case of accepting a model that is not a good representation of the processes but which fits within the errors in the calibration data (Beven, 2012; Beven and Smith, 2015). It should also be noted that the normalized scores are also based on estimates of the 95% limits around each observation (see 2.4) and therefore the potential range of uncertainty could be larger. In order to test the effect of this on model evaluation, we performed the same analysis of relaxing the scores until 1057 simulations were accepted. However, in this instance we only required the model to fit the limits at 95% of the time-steps. Figure 11 shows the time series of discharge and TP compared to the observations and shows that when accounting for the model only fitting the time-steps 95% of the time, the model still produces simulations where the peaks are underestimated, such as in early January 2013. Hence, there is the still the risk of poor models being accepted due to uncertainty in the calibration data.

**Figure 11: Generalized Likelihood Uncertainty Estimation (GLUE) weighted prediction bounds (green shading) for discharge (a) and total phosphorus loads (b) for Newby Beck outlet (part of the calibration period) based on normalized scores on both discharge and total phosphorus (TP) load evaluation measures when criteria set over 95% of time steps (1057 simulations). The black line in each plot shows the observed discharge (a) and TP loads (b), respectively.**

When the lesser constraint of just high and low flows (often the periods of most nutrient transport in flashy catchments (Haygarth et al., 2005; Ockenden et al., 2016; Perks et al., 2015)) was applied simulations that match the peaks and low flow periods with a greater degree of accuracy were produced. This also required less relaxation of the limits of acceptability (± 5.30). This is in agreement with the recent work of (Coxon et al., 2014) showing that the performance of behavioural models accepted using different diagnostics can be strongly linked to the dominant processes occurring in the catchment. In this case, we have shown that constraining the models on high and low flow periods only in a flashy catchment produces a model ensemble that captures the peak discharges and TP loads better. However, the utilization of this diagnostic further highlights the time-steps resulting in poor model performance, where time-steps not used in the evaluation (e.g. the rising and falling time-steps) return much higher normalized scores (in excess of 30 as shown in Figure 5) than when the metric across all time-steps is used.

However, we have shown here that, despite the choice of evaluation metric, a consistent picture emerges about which class of time-step is contributing most to model failures (Figure 8). Overall, the falling limb/recession time-steps were consistently a constraint on model performance contributing between 30-50% of failing time-steps for discharge and TP time-steps across both evaluation measures. This therefore indicates potential errors in the model structure of SWAT of the representation of sub-surface processes, an area of the model that has been shown to perform poorly in the past (Guse et al., 2014).

For a large number of the parameters, it is difficult to identify any sensitivity in fitting the observations, and a large amount of equifinality is evident (Figures 7 and 8). This is particularly the case for the SOL_ORGP (soil organic P) and SOL_LABP (soil labile P) parameters, which show no clear sensitivity at all using the likelihood measure based on the limits of acceptability. Both of these parameters have been shown to play an important role in

the amount of P in the water course and are often very difficult to measure in any detail at the catchment scale (Schoumans et al., 2009). It is accepted that given a 39 dimension parameter space, 5,000,000 SWAT runs provides only a small sample of the model parameter space, albeit many more than any previously published SWAT calibration exercise, and that such a small sample can contribute to the uncertainty. Thus, there is the possibility of missing potentially behavioral models during the sampling process. They are clearly, however, sparsely distributed even with the relaxed limits of acceptability. Further adding to model parameter uncertainty is the GW_DELAY parameter, which exhibits strong identifiability, but showing the identification behavioural models at both extremes of the parameter range. Therefore in this application of SWAT both high and low groundwater delay times produce equivalent model performance in terms of the relaxed limits of acceptability. This infers that there could be compensation processes occurring in the sub-surface module of the model or could highlight additional issues in the model structural representation of groundwater attenuation in the catchment.

The limits of acceptability approach provides advantages over more traditional evaluation metrics such as NSE and root mean square error (RMSE). These are global measures, which tend to focus on the average error from the data over the calibration period, rather than focus on the individual time-steps that are causing the model to fail. The limits approach utilizes the high frequency data to provide a more detailed evaluation of the model and allows the identification of critical time-steps that are causing poor model performance. Further to this, the limits approach goes someway to accounting for uncertainty in the data/observations used to calibrate the model.

However, it is impossible to make this method completely objective due to the difficulty in accounting for error in the model inputs. In past applications of the GLUE limits of acceptability approach (Liu et al., 2009) the relaxation of the limits was justified to account

for uncertainty in the model input data. However, in this case the model user must examine the degree of relaxation in the scores and utilize the available knowledge of the inputs to see if the level of relaxation is acceptable. Given the epistemic nature of the input uncertainties, it is difficult to truly assess the effect of input error and its representation needs to be independent of the model structure (e.g. Beven, 2006). One method is to employ the use of an statistical error model to account for input error in the model (e.g. Krueger et al. (2010), go some way to accounting for this) but it is difficult to create a realistic error model, even for rainfall inputs. It would also be even more computationally expensive and thus was not implemented in the present work.

The effects of both input error and model structural errors should be seen in the deviations outside the normalised limits. The results show that the limits have to be relaxed by a very large amount (up to a factor of 6.72) to gain a set of behavioral simulations that allows the sensitivity of the parameter sets to be explored. An examination of the potential input errors to the catchment system has been taken in this study to determine whether a relaxation by factors of up to seven are acceptable. In the Newby Beck catchment, there are four rain gauges sited in a relatively small area (12.5 $km^2$ – Figure 1). It is still possible that some rainfall in the catchment could be missed in the model input, particularly during summer convective storms, leading to commensurability issues with the rainfall input (Beven and Smith, 2015; Beven et al., 2011). Different rainfall input realizations and associated errors have previously been shown to impact model performance (Blazkova and Beven, 2009). However, due to the relatively good coverage by the rain gauges in the Newby Beck catchment, errors in the rainfall input are likely to be small. It can therefore be concluded that it is model structural error, rather than input error, that is leading to the high relaxation of the limits required to define model realisations of the hydrograph as acceptable.

With respect to P, there is a much larger uncertainty in the overall inputs into the catchment, particularly to the exact amounts of fertilizer spread on the land and the amount of dung deposited from grazing. Lacking more detailed information, the inputs used in this application of SWAT are based upon Defra recommendations (Defra, 2013) and local knowledge of the catchment. Furthermore, the lumped nature of the SWAT model requires average P inputs for each HRU, which can add further uncertainty in the amount of nutrients added to the system. This can therefore lead to the locations of the inputs being smoothed out leading to commensurability issues. However, the average amount of P added to the catchment per year during the run (2.3 kg $ha^{-1}$) is much smaller than the levels of P in the soil stores during the course of the run (approximately 15000 kg $ha^{-1}$). Thus, errors in P inputs and timing are unlikely to have an effect on the levels of P being transported to the stream compared to uncertainty and errors in the parameters and model structures, which govern the mobilisation and transport of P in the soil. Previous work on similar small-sized catchments also suggests that hydrological and biochemical processes have a much larger control on the temporal variations in stream P in the catchment, rather than the timings and magnitudes of the agricultural inputs (Dupas et al., 2015; Haygarth et al., 2012). In this work, we explicitly account for the uncertainty in soil P by varying the SOL_ORGP and SOL_LABP (organic and labile P soil stores) as part of the GLUE analysis with both of these parameters showing high equifinality. It has also been shown in previous analysis on Newby Beck (Ockenden et al., 2016), that the observed TP loads during storm events in the catchment are highly correlated with peaks in rainfall. These storm events account for approximately 83% of the annual TP load indicating that rainfall plays a strong role in controlling the transport of TP into the stream network. As discussed above, the errors in rainfall are likely to be relatively low in this catchment, and given its importance as a driver of TP transport along with the small contribution of P inputs to overall soil P, we can conclude that relaxing the limits by a

factor of 6.72 is not acceptable in this application of SWAT to Newby Beck. We can therefore conclude that, as with discharge, model structural error is the likely cause of this requirement to relax the constraints by such a substantial amount.

The ability of the model to adequately simulate the observed TP loads is also further compounded by the poor performance of SWAT in terms of discharge evaluation, given that discharge is part of the TP load calculation. Hence, as model structural error has been shown to be such a large constraint in the accurate prediction of discharge and thus TP loads, it is unlikely that improvements in input data will greatly improve model predictions. In addition to this, even in a small experimental catchment, gaining sufficient improvement in model input data would require significant expense. In the case of TP, this would require detailed farmer logs in timings and location of fertilizer applications, detailed monitoring of surface and subsurface storage and availability of TP in the catchment, along with detailed field scale budgets of the nutrients in the soils.

This prompts an additional question, if we are required to relax the limits, which are primarily due to structural error in the model, by a factor of 6.72, should we go to the expense of collecting the additional input data required by such a complex model structure? It has been shown in previous work (Dean et al., 2009; Shen et al., 2012a) that insufficient input data are a constraint on even the best of models, therefore clearly improvement is required on both sides. The advantage of using the limits of acceptability approach is that we can use the results of the model evaluation to target which areas of the model structure require improvement and infer which areas are best to target our efforts for additional data collection, particularly in situations where funds for such efforts are limited.

## 5 Conclusions

This study has presented the first 'limits of acceptability' assessment of the SWAT model using continuous high frequency discharge and water quality monitoring data. We highlight that having the availability of high frequency data coupled with the GLUE 'limits of acceptability' approach; the model performance can be assessed taking into account the uncertainty on the calibration data at each time-step. This provides greater insights into why the model is failing beyond the more traditional global measures of model evaluation such as NSE and RMSE.

In the application of SWAT to the Newby Beck headwater catchment in the UK, it is shown that the limits of acceptability based on output observational uncertainties have to be relaxed by a substantial amount (by factors of between 5.3 and 6.72 on a normalized scale depending on the evaluation criteria used) in order to produce a set of behavioral simulations (1001 and 1016 respectively out of 5,000,000 realizations) on which to perform model diagnostics. In this case, despite the evaluation metric used, the model is shown to consistently perform poorly during periods of recession in both the discharge and TP time series, with uncertainty in the representation of subsurface flow pathways identified as a potential cause for this poor performance. During the validation period the model was shown to capture the timings of peaks in the river TP load, however, it was shown to often predict the magnitude of these peaks poorly. This work raises an interesting point- how much relaxation is allowable in the limits of acceptability before we consider the model as not providing useful predictions of the processes occurring in the catchment? On the one hand, we have learnt from the model to identify areas where we need to focus future model development and data collection efforts in river catchments. On the other, we have shown that in this particular case, SWAT is not fit for purpose to be used as a management tool due to the large uncertainty bounds on predictions, particularly during the validation period. This conclusion agrees with previous applications of SWAT to other catchments of similar

catchment areas and similar geoclimatic circumstances (Hoang et al., 2017; Moges et al., 2017; Schneiderman et al., 2007). Therefore, despite being used in numerous catchments worldwide (often with less rigorous evaluation), SWAT may not be fit for purpose as a general management tool, particularly in flashy catchments being dominated by overland flow where the model structure may be inadequate to accurately capture the major catchment processes dominating P transfer.

However, there is still a need to advise policy makers on how changes in the environment are likely to affect hydrology and water quality in the future and what mitigation measures to take, if any. A number of potential options are available, such as precautionary methods suggested by Beven (2011), or the use of fuzzy modelling methods (Page et al., 2012; Zhang et al., 2013) or finding another process based model to use – though it is highly likely that another model will suffer the same uncertainty issues as shown here with SWAT. A final option is to shift towards more simple P transfer model (E.g. Dupas et al. (2016)) which have been shown to capture P losses well with minimum input data. However as highlighted by Dupas et al. (2016), such models still have uncertainties associated with them and in some cases still require substantial relaxation of the 'limits of acceptability'.

We acknowledge that process-based models may be potentially useful catchment management tools. They are often used to quantify the effects of changes in catchment conditions (e.g. climate change) on the behavior of nutrients in catchments (Crossman et al., 2014; Wang and Sun, 2016). They are primarily used because they provide a numerical representation of conceptual processes that in theory represent how these processes adapt to changing environmental conditions under different scenarios. However, the results presented here stress the importance of having the best available input data along with high frequency data from continuous monitoring systems for rigorous model evaluation, as highlighted in previous studies (Benettin et al., 2015; Dupas et al., 2016; Halliday et al., 2015; Ockenden et

al., 2017). High frequency data allows us to set more robust 'limits of acceptability', particularly in catchments with a flashy response where infrequent grab samples may fail to capture key processes/events and may not provide a stringent enough test of the model structure/processes. The results also imply that more needs to be done to improve the ability of the model to simulate the dynamics of key catchment processes with parameters that are more identifiable in practical applications, or more easily estimated in predicting future conditions. Finally, our results also indicate the possibility that even with the best representation of the key processes in the model structure; we still may have a long way to go to have sufficient input data to adequately drive such complex model structures.

The study has not resolved the issue of how far the limits of acceptability should be relaxed to provide a set of models considered useful for predicting outcomes. That is a question for individual users to consider for particular types of applications, i.e. can we be objective about the effects of input error on model performance, particularly for predicting nutrient responses? This study suggests that SWAT may not be fit-for-purpose in this particular application, however, confirmation of its general applicability, or not, requires critical testing of the method on multiple models and multiple catchment datasets in ways that allow for uncertainty and potential equifinality of model representations.

**Acknowledgments**

This study was funded by the Natural Environment Research Council (NERC) as part of the NUTCAT 2050 project, grants NE/K002392/1, NE/K002430/1 and NE/K002406/1, and supported by the Joint UK BEIS/Defra Met Office Hadley Centre Climate Programme (GA01101). The authors are grateful to the Eden Demonstration Test Catchment (Eden DTC) research platform for provision of the field data (Department for Environment, Food and Rural Affairs (Defra), projects WQ0210, WQ0211, WQ0212 and LM0304). The data

used in this study are openly available from the Lancaster University data archive (details reserved until publication). The DTC data are available from the Eden DTC consortium until the data archive is transferred to Defra (Department for Environment, Food & Rural Affairs) as the holding body. The SWAT model executable and source code are open source and are available for download at http://swat.tamu.edu/.

**References**

Arnold, J.G. et al., 2012. Swat: Model Use, Calibration, and Validation. Transactions of the Asabe, 55(4): 1491-1508.

Arnold, J.G., Srinivasan, R., Muttiah, R.S., Williams, J.R., 1998. Large area hydrologic modeling and assessment - Part 1: Model development. Journal of the American Water Resources Association, 34(1): 73-89. DOI:10.1111/j.1752-1688.1998.tb05961.x

Arnold, J.G., Williams, J.R., Maidment, D.R., 1995. Continuous-time water and sediment routing model for large basins. Journal of Hydraulic Engineering-Asce, 121(2): 171-183. DOI:10.1061/(asce)0733-9429(1995)121:2(171)

Benettin, P., Kirchner, J.W., Rinaldo, A., Botter, G., 2015. Modeling chloride transport using travel time distributions at Plynlimon, Wales. Water Resour. Res., 51(5): 3259-3276. DOI:10.1002/2014WR016600

Beven, K., 1996. A discussion of distributed hydrological modelling. In: JC, M.B.R.A. (Ed.), Distributed hydrological modelling. Kluwer, Netherlands, pp. 255-278.

Beven, K., 2002. Towards an alternative blueprint for a physically based digitally simulated hydrologic response modelling system. Hydrological Processes, 16(2): 189-206. DOI:10.1002/hyp.343

Beven, K., 2006. A manifesto for the equifinality thesis. J. Hydrol., 320(1-2): 18-36. DOI:10.1016/j.jhydrol.2005.07.007

Beven, K., 2009. Environmental modelling: an uncertain future? Routledge, London.

Beven, K., 2011. I believe in climate change but how precautionary do we need to be in planning for the future? Hydrological Processes, 25(9): 1517-1520. DOI:10.1002/hyp.7939

Beven, K., 2012. Rainfall-runoff modelling: the primer. Wiley-Blackwell, Chichester.

Beven, K., Binley, A., 1992. The future of distributed models - model calibration and uncertainty prediction. Hydrological Processes, 6(3): 279-298. DOI:10.1002/hyp.3360060305

Beven, K., Binley, A., 2014. GLUE: 20 years on. Hydrological Processes, 28(24): 5897-5918. DOI:10.1002/hyp.10082

Beven, K., Smith, P., 2015. Concepts of Information Content and Likelihood in Parameter Calibration for Hydrological Simulation Models. J. Hydrol. Eng., 20(1): 15. DOI:10.1061/(asce)he.1943-5584.0000991

Beven, K., Smith, P.J., Wood, A., 2011. On the colour and spin of epistemic error (and what we might do about it). Hydrology and Earth System Sciences, 15(10): 3123-3133. DOI:10.5194/hess-15-3123-2011

Blazkova, S., Beven, K., 2009. A limits of acceptability approach to model evaluation and uncertainty estimation in flood frequency estimation by continuous simulation: Skalka catchment, Czech Republic. Water Resour. Res., 45: 12. DOI:10.1029/2007wr006726

Bosch, N.S., Evans, M.A., Scavia, D., Allan, J.D., 2014. Interacting effects of climate change and agricultural BMPs on nutrient runoff entering Lake Erie. J. Gt. Lakes Res., 40(3): 581-589. DOI:10.1016/j.jglr.2014.04.011

Brakensiek, D.L., 1967. Kinematic Flood Routing. Transactions of the ASAE, 10(3): 340-343.

Brown, L.C., Barnwell Jr., T.O., 1987. The enhanced water quality models QUAL2E and QUAL2E- UNCAS: Documentation and user manual. EPA document EPA/600/3- 87/007., USEPA, Athens GA.

Coxon, G., Freer, J., Wagener, T., Odoni, N.A., Clark, M., 2014. Diagnostic evaluation of multiple hypotheses of hydrological behaviour in a limits-of-acceptability framework for 24 UK catchments. Hydrological Processes, 28(25): 6135-6150. DOI:10.1002/hyp.10096

Coxon, G. et al., 2015. A novel framework for discharge uncertainty quantification applied to 500 UK gauging stations. Water Resour. Res., 51(7): 5531-5546. DOI:10.1002/2014wr016532

Cranfield University, 2014. The Soils Guide, Cranfield University.

Crossman, J. et al., 2013. Impacts of climate change on hydrology and water quality: Future proofing management strategies in the Lake Simcoe watershed, Canada. J. Gt. Lakes Res., 39(1): 19-32. DOI:10.1016/j.jglr.2012.11.003

Crossman, J. et al., 2014. Flow pathways and nutrient transport mechanisms drive hydrochemical sensitivity to climate change across catchments with different geology and topography. Hydrol. Earth Syst. Sci., 18(12): 5125-5148. DOI:10.5194/hess-18-5125-2014

Dean, S., Freer, J., Beven, K., Wade, A.J., Butterfield, D., 2009. Uncertainty assessment of a process-based integrated catchment model of phosphorus. Stoch. Environ. Res. Risk Assess., 23(7): 991-1010. DOI:10.1007/s00477-008-0273-z

Defra, 2013. The British Fertiliser survey of fertiliser practice. Fertiliser use on farm crops for crop year 2012.

Dupas, R., Gascuel-Odoux, C., Gilliet, N., Grimaldi, C., Gruau, G., 2015. Distinct export dynamics for dissolved and particulate phosphorus reveal independent transport mechanisms in an arable headwater catchment. Hydrological Processes, 29(14): 3162-3178. DOI:10.1002/hyp.10432

Dupas, R. et al., 2016. Uncertainty assessment of a dominant-process catchment model of dissolved phosphorus transfer. Hydrol. Earth Syst. Sci., 20(12): 4819-4835. DOI:10.5194/hess-20-4819-2016

El-Khoury, A. et al., 2015. Combined impacts of future climate and land use changes on discharge, nitrogen and phosphorus loads for a Canadian river basin. Journal of Environmental Management, 151: 76-86. DOI:10.1016/j.jenvman.2014.12.012

European Union, 2000. Directive 2000/60/EC: Establishing a framework for Community action in the field of water policy (The Water Framework Directive).

Ewen, J., Geris, J., O'Donnell, G., Mayes, Q., O'Connell, E., 2010. Multiscale Experimentation, Moitoring and Analysis of Long-term Land Use Changes and Flood Risk - SC060092: Final Science Report, Newcastle University, Newcastle-Upon-Tyne.

Freer, J.E., McMillan, H., McDonnell, J.J., Beven, K.J., 2004. Constraining dynamic TOPMODEL responses for imprecise water table information using fuzzy rule based

performance measures. J. Hydrol., 291(3–4): 254-277. DOI:https://doi.org/10.1016/j.jhydrol.2003.12.037

Gassman, P.W., Reyes, M.R., Green, C.H., Arnold, J.G., 2007. The soil and water assessment tool: Historical development, applications, and future research directions. Transactions of the Asabe, 50(4): 1211-1250.

Guse, B., Reusser, D.E., Fohrer, N., 2014. How to improve the representation of hydrological processes in SWAT for a lowland catchment – temporal analysis of parameter sensitivity and model performance. Hydrological Processes, 28(4): 2651-2670. DOI:10.1002/hyp.9777

Halliday, S.J. et al., 2015. High-frequency water quality monitoring in an urban catchment: hydrochemical dynamics, primary production and implications for the Water Framework Directive. Hydrological Processes, 29(15): 3388-3407. DOI:10.1002/hyp.10453

Harmel, R.D. et al., 2014. Evaluating, interpreting, and communicating performance of hydrologic/water quality models considering intended use: A review and recommendations. Environ. Modell. Softw., 57: 40-51. DOI:10.1016/j.envsoft.2014.02.013

Haygarth, P.M. et al., 2012. Scaling up the phosphorus signal from soil hillslopes to headwater catchments. Freshwater Biology, 57: 7-25. DOI:10.1111/j.1365-2427.2012.02748.x

Haygarth, P.M., Wood, F.L., Heathwaite, A.L., Butler, P.J., 2005. Phosphorus dynamics observed through increasing scales in a nested headwater-to-river channel study. Sci. Total Environ., 344(1-3): 83-106. DOI:10.1016/j.scitotoenv.2005.02.007

Hoang, L. et al., 2017. Predicting saturation-excess runoff distribution with a lumped hillslope model: SWAT-HS. Hydrological Processes, 31(12): 2226-2243. DOI:10.1002/hyp.11179

Intermap Technologies, 2009. NEXTMap British Digital Terrain (DTM) Model Data by Intermap. NERC Earth Observation Data Centre.

Izaurralde, R.C., Williams, J.R., McGill, W.B., Rosenberg, N.J., Jakas, M.C.Q., 2006. Simulating soil C dynamics with EPIC: Model description and testing against long-term data. Ecological Modelling, 192(3-4): 362-384. DOI:10.1016/j.ecolmodel.2005.07.010

Jin, L. et al., 2015. Assessing the impacts of climate change and socio-economic changes on flow and phosphorus flux in the Ganga river system. Environ. Sci.-Process Impacts, 17(6): 1098-1110. DOI:10.1039/c5em00092k

Johnes, P.J., 2007. Uncertainties in annual riverine phosphorus load estimation: Impact of load estimation methodology, sampling frequency, baseflow index and catchment population density. J. Hydrol., 332(1-2): 241-258. DOI:10.1016/j.jhydrol.2006.07.006

Jones, P., Harpham, C., Kilsby, G.C., Glenis, V., Burton, A., 2010. UK Climate Projections science report: Projections of future daily climate for the UK from the Weather Generator, Met Office, UK.

Karamouz, M., Taheriyoun, M., Seyedabadi, M., Nazif, S., 2015. Uncertainty based analysis of the impact of watershed phosphorus load on reservoir phosphorus concentration. J. Hydrol., 521: 533-542. DOI:10.1016/j.jhydrol.2014.12.028

Kendon, E.J. et al., 2014. Heavier summer downpours with climate change revealed by weather forecast resolution model. Nat. Clim. Chang., 4(7): 570-576. DOI:10.1038/nclimate2258

Knisel, W.G., 1980. CREAMS: A field scale model for chemical, runoff, and erosion from agricultural management system, Conservation Research Report No. 26, U.S. Department of Agriculture, Washington DC.

Krueger, T., Freer, J., Quinton, J.N., Macleod, C.J.A., 2007. Processes affecting transfer of sediment and colloids, with associated phosphorus, from intensively farmed grasslands: a critical not on modelling phosphorus transfers. Hydrological Processes, 21(4): 557-562. DOI:10.1002/hyp.6596

Krueger, T. et al., 2010. Ensemble evaluation of hydrological model hypotheses. Water Resour. Res., 46(7): n/a-n/a. DOI:10.1029/2009WR007845

Krueger, T. et al., 2009. Uncertainties in Data and Models to Describe Event Dynamics of Agricultural Sediment and Phosphorus Transfer All rights reserved. No part of this periodical may be reproduced or transmitted in any form or by any means, electronic or mechanical, including photocopying, recording, or any information storage and retrieval system, without permission in writing from the publisher. J. Environ. Qual., 38(3): 1137-1148. DOI:10.2134/jeq2008.0179

Krueger, T. et al., 2012. Comparing empirical models for sediment and phosphorus transfer from soils to water at field and catchment scale under data uncertainty. European Journal of Soil Science, 63(2): 211-223. DOI:10.1111/j.1365-2389.2011.01419.x

Leonard, R.A., Knisel, W.G., Still, D.A., 1987. GLEAMS - Groundwater Loading Effects of Agricultural Management-Systems. Transactions of the Asae, 30(5): 1403-1418.

Liu, Y.L., Freer, J., Beven, K., Matgen, P., 2009. Towards a limits of acceptability approach to the calibration of hydrological models: Extending observation error. J. Hydrol., 367(1-2): 93-103. DOI:10.1016/j.jhydrol.2009.01.016

Macleod, C.J.A., Falloon, P.D., Evans, R., Haygarth, P.M., 2012. The Effects of Climate Change on the Mobilization of Diffuse Substances from Agricultural Systems. In: Sparks, D.L. (Ed.), Advances in Agronomy, Vol 115. Advances in Agronomy, pp. 41-77. DOI:10.1016/b978-0-12-394276-0.00002-0

McGonigle, D.F. et al., 2014. Developing Demonstration Test Catchments as a platform for transdisciplinary land management research in England and Wales. Environ. Sci.-Process Impacts, 16(7): 1618-1628. DOI:10.1039/c3em00658a

McMillan, H., Krueger, T., Freer, J., 2012. Benchmarking observational uncertainties for hydrology: rainfall, river discharge and water quality. Hydrological Processes, 26(26): 4078-4111. DOI:10.1002/hyp.9384

McMillan, H.K., Westerberg, I.K., 2015. Rating curve estimation under epistemic uncertainty. Hydrological Processes, 29(7): 1873-1882. DOI:10.1002/hyp.10419

Met Office, 2012. Met Office Integrated Data Archive System (MIDAS) Land and Marine Surface Stations Data (1853-current). . In: NCAS British Atmospheric Data Centre (Ed.).

Moges, M.A. et al., 2017. Suitability of Watershed Models to Predict Distributed Hydrologic Response in the Awramba Watershed in Lake Tana Basin. Land Degradation & Development, 28(4): 1386-1397. DOI:10.1002/ldr.2608

Monteith, J.L., 1965. Evaporation and the environment, The state and movement of water in living organisms. 19th Symposia of the Society for Experimental Biology. Cambridge University Press, London, pp. 205-234.

Morton, D. et al., 2011. Final Report for LCM2007 - the new UK Land Cover Map.

Neitsch, S.L., Arnold, J.G., Kiniry, J.R., Williams, J.R., 2011. Soil and Water Assessment Tool Theoretical Documentation, Version 2009, Texas Water Resources Institute, Temple.

Ockenden, M.C. et al., 2016. Changing climate and nutrient transfers: Evidence from high temporal resolution concentration-flow dynamics in headwater catchments. Sci. Total Environ., 548: 325-339. DOI:10.1016/j.scitotenv.2015.12.086

Ockenden, M.C. et al., 2017. Major agricultural changes required to mitigate phosphorus losses under climate change. Nature Communications, 8(1): 161. DOI:10.1038/s41467-017-00232-0

Outram, F.N. et al., 2014. High-frequency monitoring of nitrogen and phosphorus response in three rural catchments to the end of the 2011–2012 drought in England. Hydrol. Earth Syst. Sci., 18(9): 3429-3448. DOI:10.5194/hess-18-3429-2014

Overton, D.E., 1966. Muskingum flood routing of upland streamflow. J. Hydrol., 4: 185-200. DOI:http://dx.doi.org/10.1016/0022-1694(66)90079-5

Owen, G.J. et al., 2012. Monitoring agricultural diffuse pollution through a dense monitoring network in the River Eden Demonstration Test Catchment, Cumbria, UK. Area, 44(4): 443-453. DOI:10.1111/j.1475-4762.2012.01107.x

Page, T., Beven, K.J., Freer, J., Jenkins, A., 2003. Investigating the Uncertainty in Predicting Responses to Atmospheric Deposition using the Model of Acidification of Groundwater in Catchments (MAGIC) within a Generalised Likelihood Uncertainty Estimation (GLUE) Framework. Water, Air, and Soil Pollution, 142(1): 71-94. DOI:10.1023/a:1022011520036

Page, T., Beven, K.J., Freer, J., Neal, C., 2007. Modelling the chloride signal at Plynlimon, Wales, using a modified dynamic TOPMODEL incorporating conservative chemical mixing (with uncertainty). Hydrological Processes, 21(3): 292-307. DOI:10.1022/hyp.6186

Page, T., Beven, K.J., Whyatt, D., 2004. Predictive Capability in Estimating Changes in Water Quality: Long-Term Responses to Atmospheric Deposition. Water, Air, and Soil Pollution, 151(1): 215-244. DOI:10.1023/B:WATE.0000009893.66091.ec

Page, T., Heathwaite, A.L., Thompson, L.J., Pope, L., Willows, R., 2012. Eliciting fuzzy distributions from experts for ranking conceptual risk model components. Environ. Modell. Softw., 36: 19-34. DOI:http://dx.doi.org/10.1016/j.envsoft.2011.03.001

Pappenberger, F. et al., 2006. Influence of uncertain boundary conditions and model structure on flood inundation predictions. Advances in Water Resources, 29(10): 1430-1449. DOI:10.1016/j.advwatres.2005.11.012

Perks, M.T. et al., 2015. Dominant mechanisms for the delivery of fine sediment and phosphorus to fluvial networks draining grassland dominated headwater catchments. Sci. Total Environ., 523: 178-190. DOI:http://dx.doi.org/10.1016/j.scitotenv.2015.03.008

Radcliffe, D.E., Freer, J., Schoumans, O., 2009. Diffuse Phosphorus Models in the United States and Europe: Their Usages, Scales, and Uncertainties. J. Environ. Qual., 38(5): 1956-1967. DOI:10.2134/jeq2008.0060

Rankinen, K., Karvonen, T., Butterfield, D., 2006. An application of the GLUE methodology for estimating the parameters of the INCA-N model. Sci. Total Environ., 365(1-3): 123-139. DOI:10.1016/j.scitotenv.2006.02.034

Schneiderman, E.M. et al., 2007. Incorporating variable source area hydrology into a curve-number-based watershed model. Hydrological Processes, 21(25): 3420-3430. DOI:10.1002/hyp.6556

Schoumans, O.F. et al., 2009. Evaluation of the difference of eight model applications to assess diffuse annual nutrient losses from agricultural land. Journal of Environmental Monitoring, 11(3): 540-553. DOI:10.1039/B823240G

Schuol, J., Abbaspour, K.C., 2006. Calibration and uncertainty issues of a hydrological model (SWAT) applied to West Africa. Adv. Geosci., 9: 137-143. DOI:10.5194/adgeo-9-137-2006

Shen, Z.Y., Chen, L., Chen, T., 2012a. Analysis of parameter uncertainty in hydrological and sediment modeling using GLUE method: a case study of SWAT model applied to Three Gorges Reservoir Region, China. Hydrol. Earth Syst. Sci., 16(1): 121-132. DOI:10.5194/hess-16-121-2012

Shen, Z.Y., Chen, L., Liao, Q., Liu, R.M., Hong, Q., 2012b. Impact of spatial rainfall variability on hydrology and nonpoint source pollution modeling. J. Hydrol., 472: 205-215. DOI:10.1016/j.jhydrol.2012.09.019

Shen, Z.Y., Chen, L., Liao, Q., Liu, R.M., Huang, Q., 2013. A comprehensive study of the effect of GIS data on hydrology and non-point source pollution modeling. Agricultural Water Management, 118: 93-102. DOI:10.1016/j.agwat.2012.12.005

Taylor, S.D., He, Y., Hiscock, K.M., 2016. Modelling the impacts of agricultural management practices on river water quality in Eastern England. Journal of Environmental Management, 180: 147-163. DOI:http://dx.doi.org/10.1016/j.jenvman.2016.05.002

Team, R.C., 2016. R: A language and Environment for Statistical Computing., R Foundation for Statistical Computing, https://www.r-project.org/, Vienna, Austria.

van Griensven, A. et al., 2006. A global sensitivity analysis tool for the parameters of multi-variable catchment models. J. Hydrol., 324(1-4): 10-23. DOI:10.1016/j.jhydrol.2005.09.008

Vrugt, J.A., Sadegh, M., 2013. Toward diagnostic model calibration and evaluation: Approximate Bayesian computation. Water Resour. Res., 49(7): 4335-4345. DOI:10.1002/wrcr.20354

Wang, H., Sun, F., 2016. Impact of LUCC on Streamflow using the SWAT Model over the Wei River Basin on the Loess Plateau of China. Hydrol. Earth Syst. Sci. Discuss., 2016: 1-30. DOI:10.5194/hess-2016-332

Westerberg, I., Guerrero, J.L., Seibert, J., Beven, K.J., Halldin, S., 2011. Stage-discharge uncertainty derived with a non-stationary rating curve in the Choluteca River, Honduras. Hydrological Processes, 25(4): 603-613. DOI:10.1002/hyp.7848

Whitehead, P.G. et al., 2013. A cost-effectiveness analysis of water security and water quality: impacts of climate and land-use change on the River Thames system.

Philosophical Transactions of the Royal Society a-Mathematical Physical and Engineering Sciences, 371(2002). DOI:10.1098/rsta.2012.0413

Williams, J.R., 1990. The Erosion-Productivity Impact Calculator (EPIC) Model - A Case-History. Philosophical Transactions of the Royal Society of London Series B-Biological Sciences, 329(1255): 421-428. DOI:10.1098/rstb.1990.0184

Woznicki, S.A., Nejadhashemi, A.P., 2014. Assessing uncertainty in best management practice effectiveness under future climate scenarios. Hydrological Processes, 28(4): 2550-2566. DOI:10.1002/hyp.9804

Yen, H., Hoque, Y., Harmel, R.D., Jeong, J., 2015. The impact of considering uncertainty in measured calibration/validation data during auto-calibration of hydrologic and water quality models. Stoch. Environ. Res. Risk Assess., 29(7): 1891-1901. DOI:10.1007/s00477-015-1047-z

Zhang, P. et al., 2014. Uncertainty of SWAT model at different DEM resolutions in a large mountainous watershed. Water Research, 53: 132-144. DOI:10.1016/j.watres.2014.01.018

Zhang, T. et al., 2013. Estimating phosphorus delivery with its mitigation measures from soil to stream using fuzzy rules. Soil Use and Management, 29: 187-198. DOI:10.1111/j.1475-2743.2012.00433.x

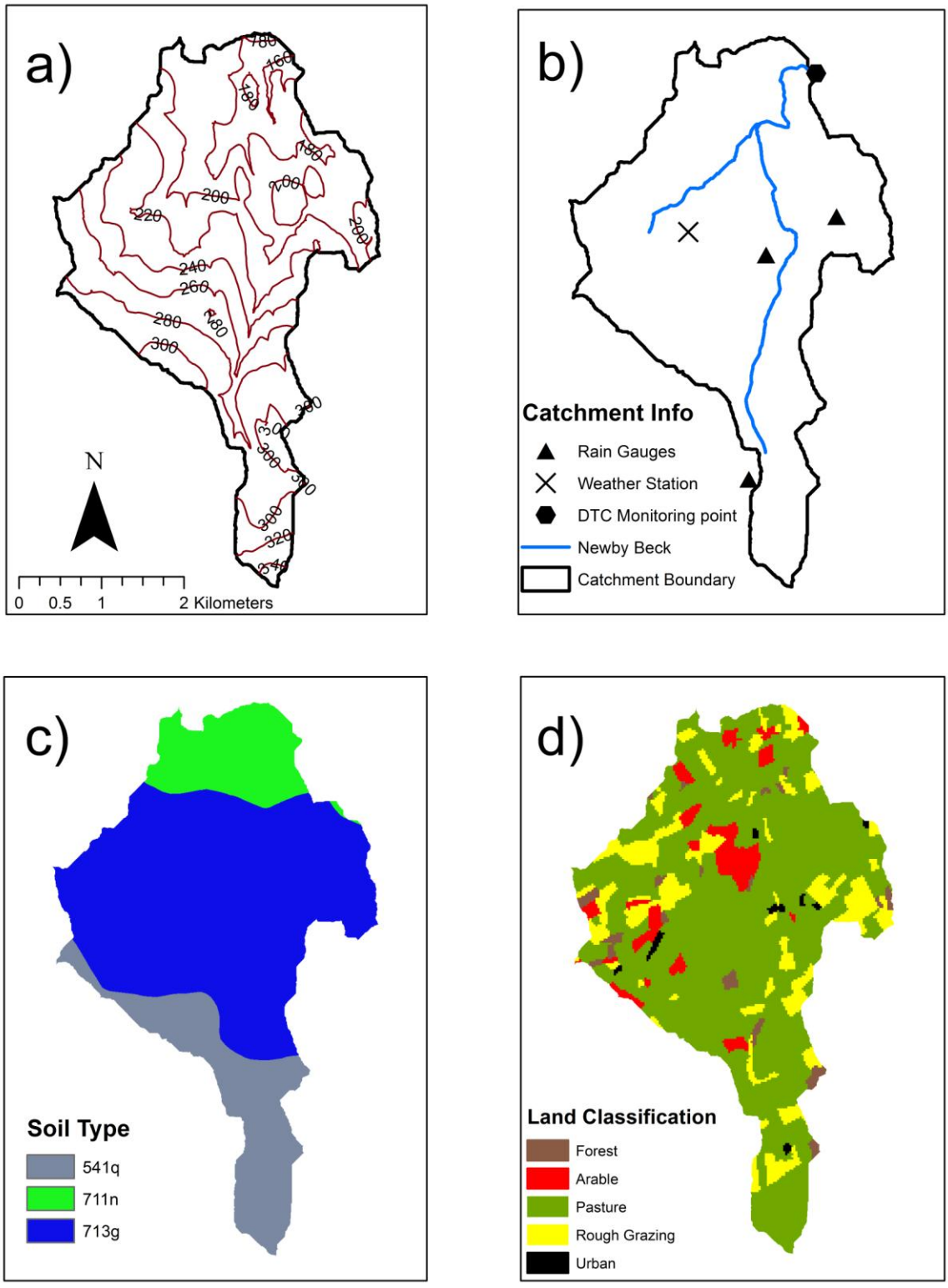
a)
160
180
200
220
240
260
280
300
320
340
360
380
N
0 0.5 1 2 Kilometers
b)
Catchment Info
Rain Gauges
Weather Station
DTC Monitoring point
Newby Beck
Catchment Boundary
c)
Soil Type
541q
711n
713g
d)
Land Classification
Forest
Arable
Pasture
Rough Grazing
Urban

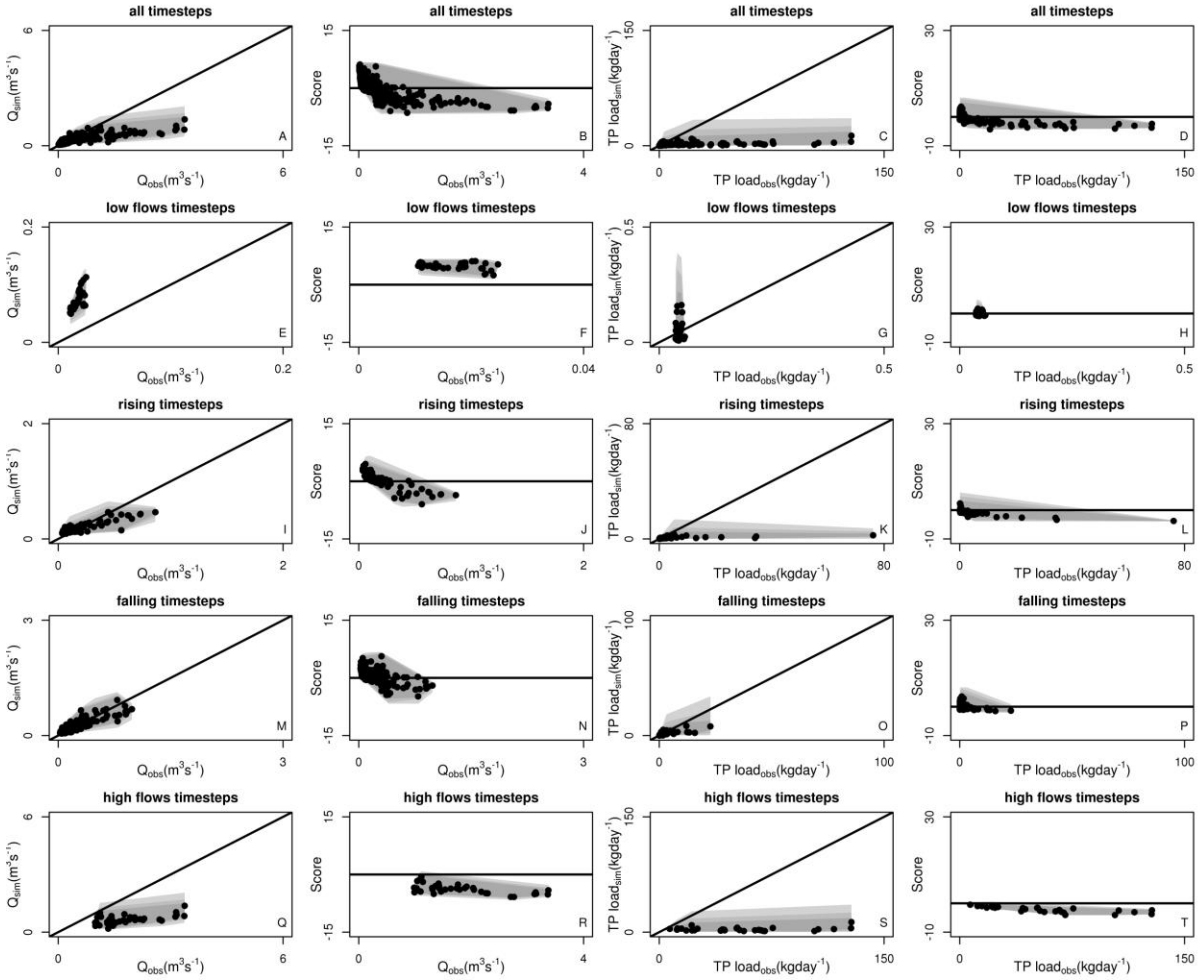

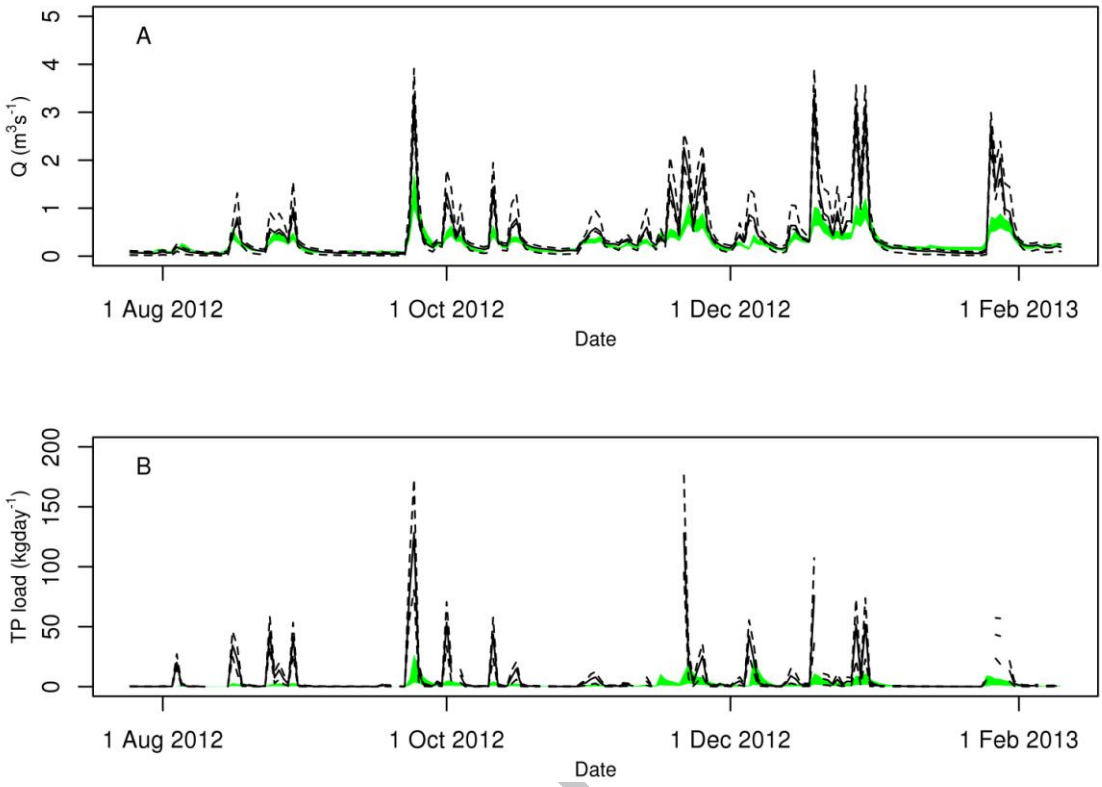

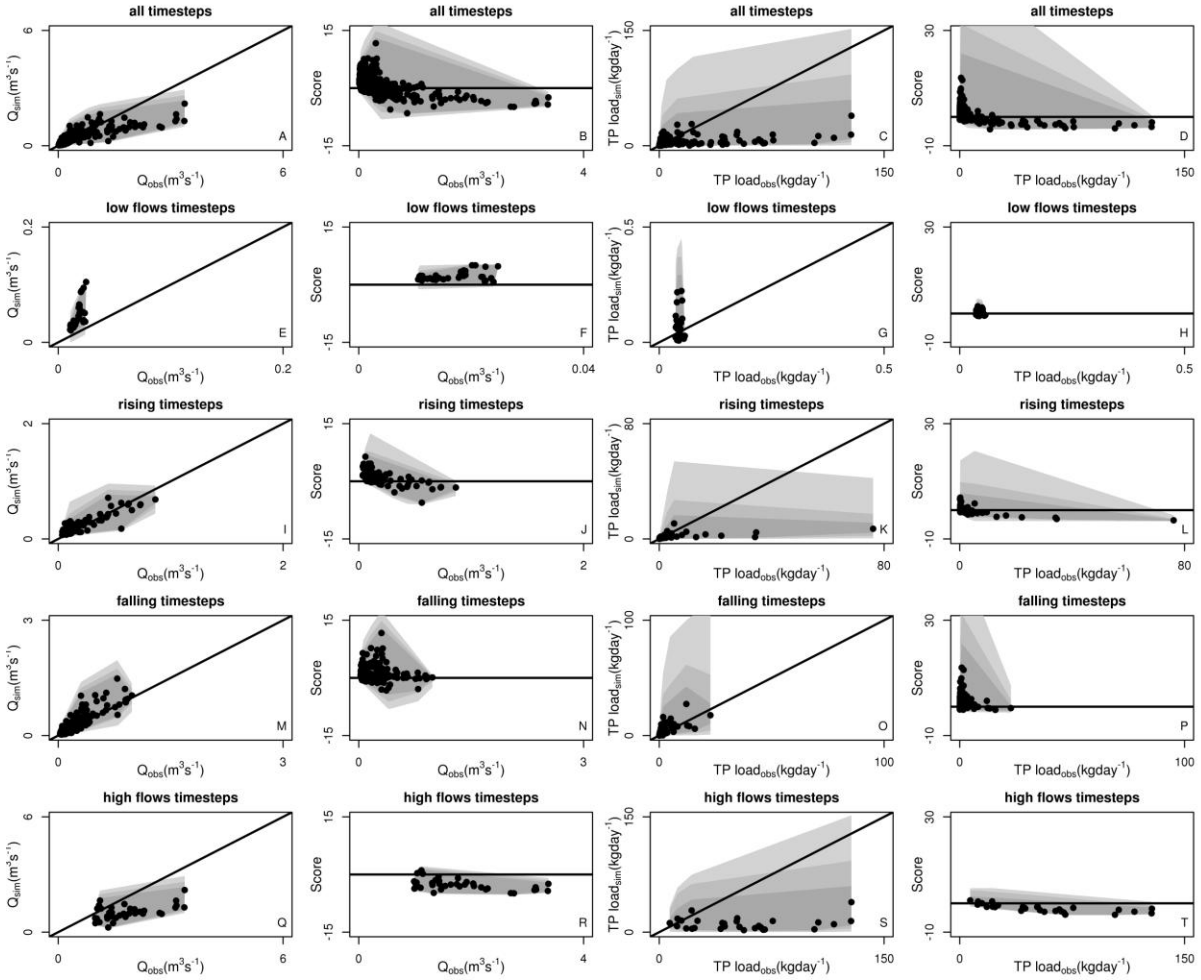

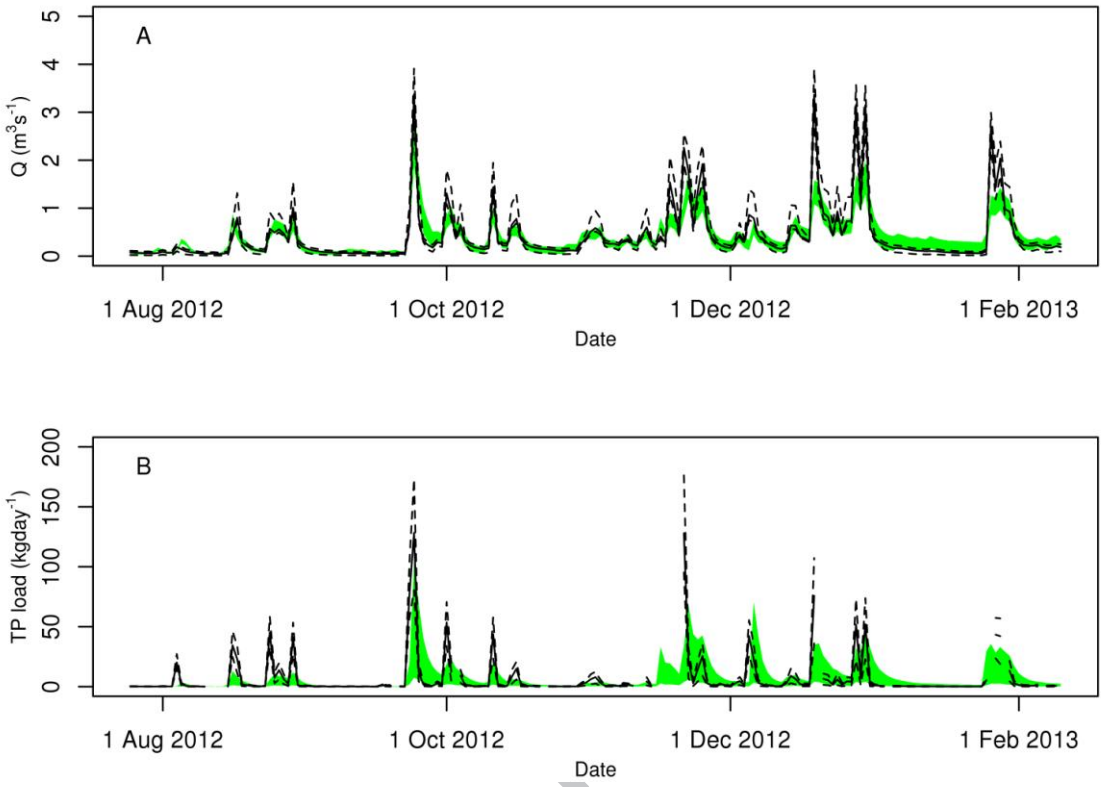

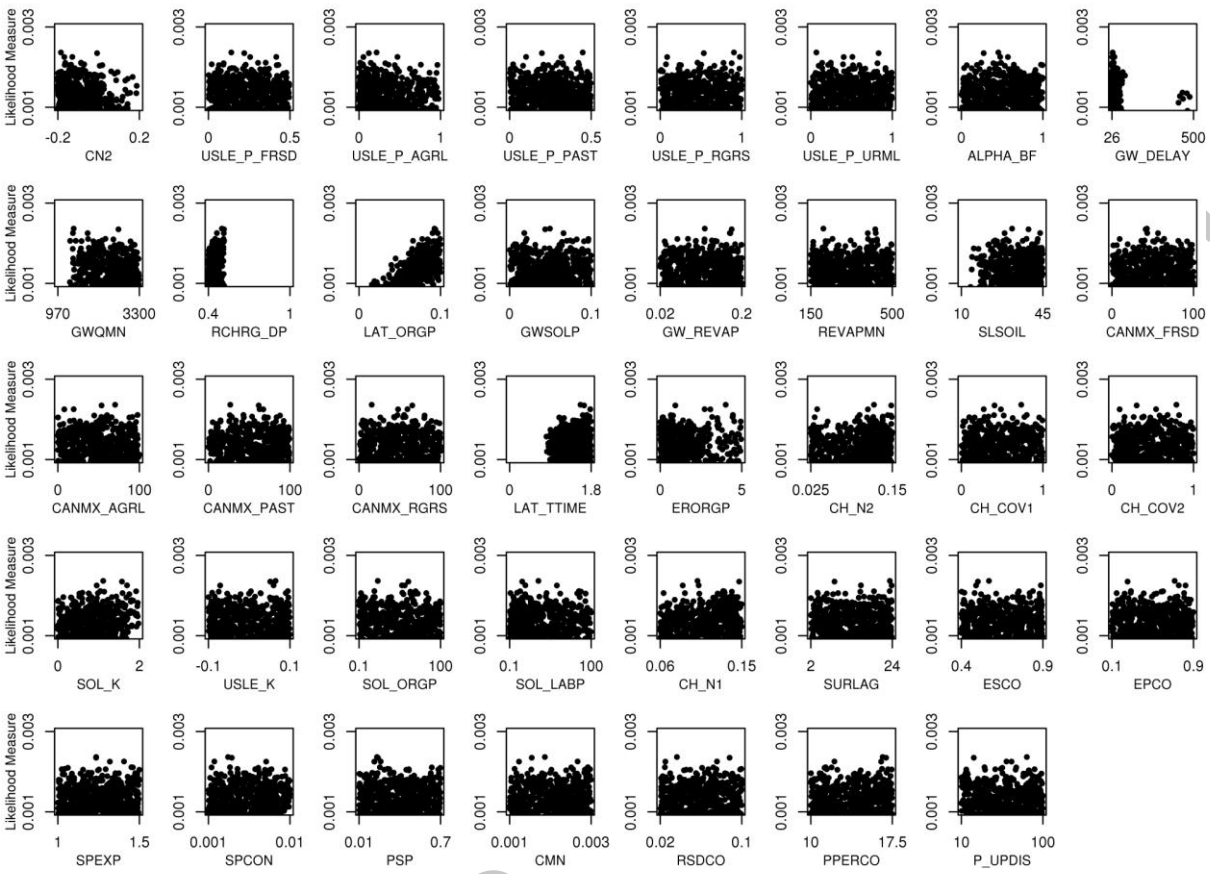

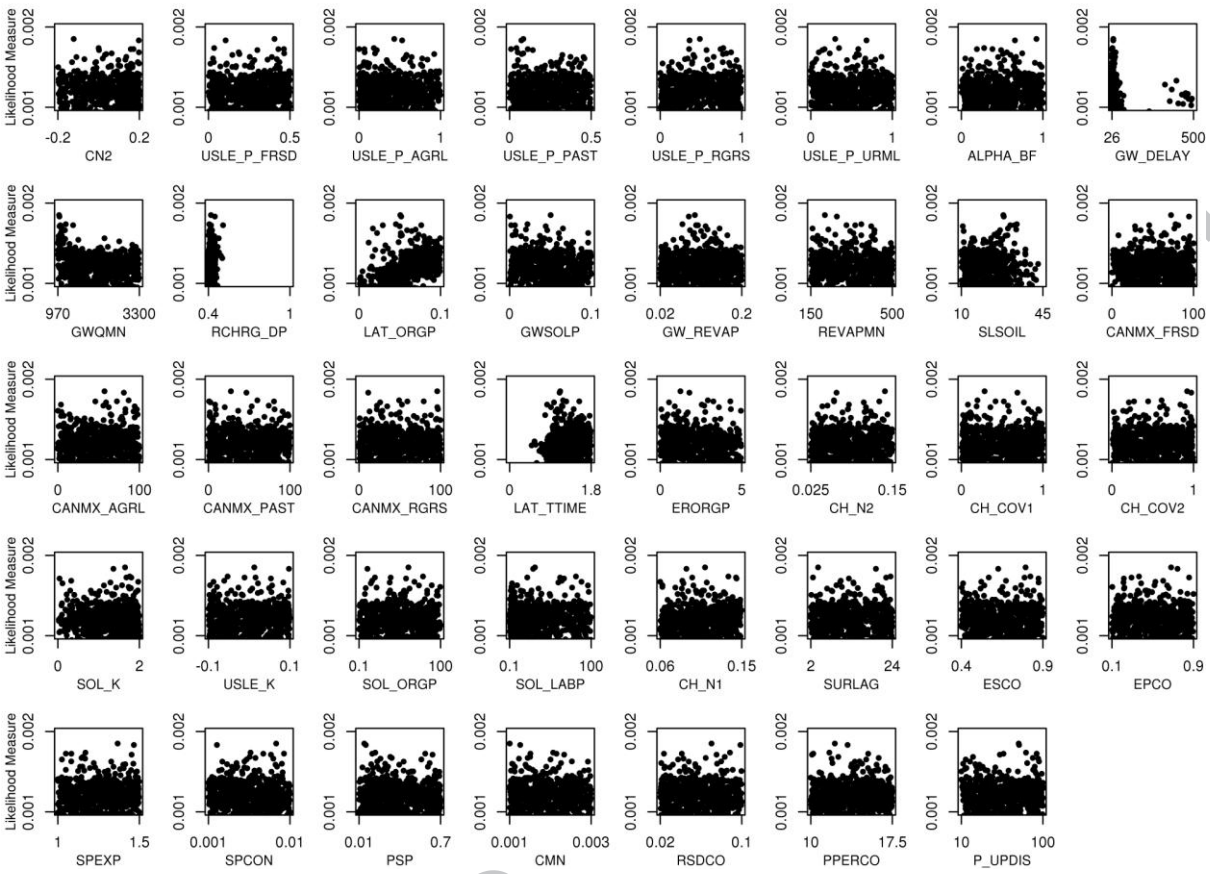

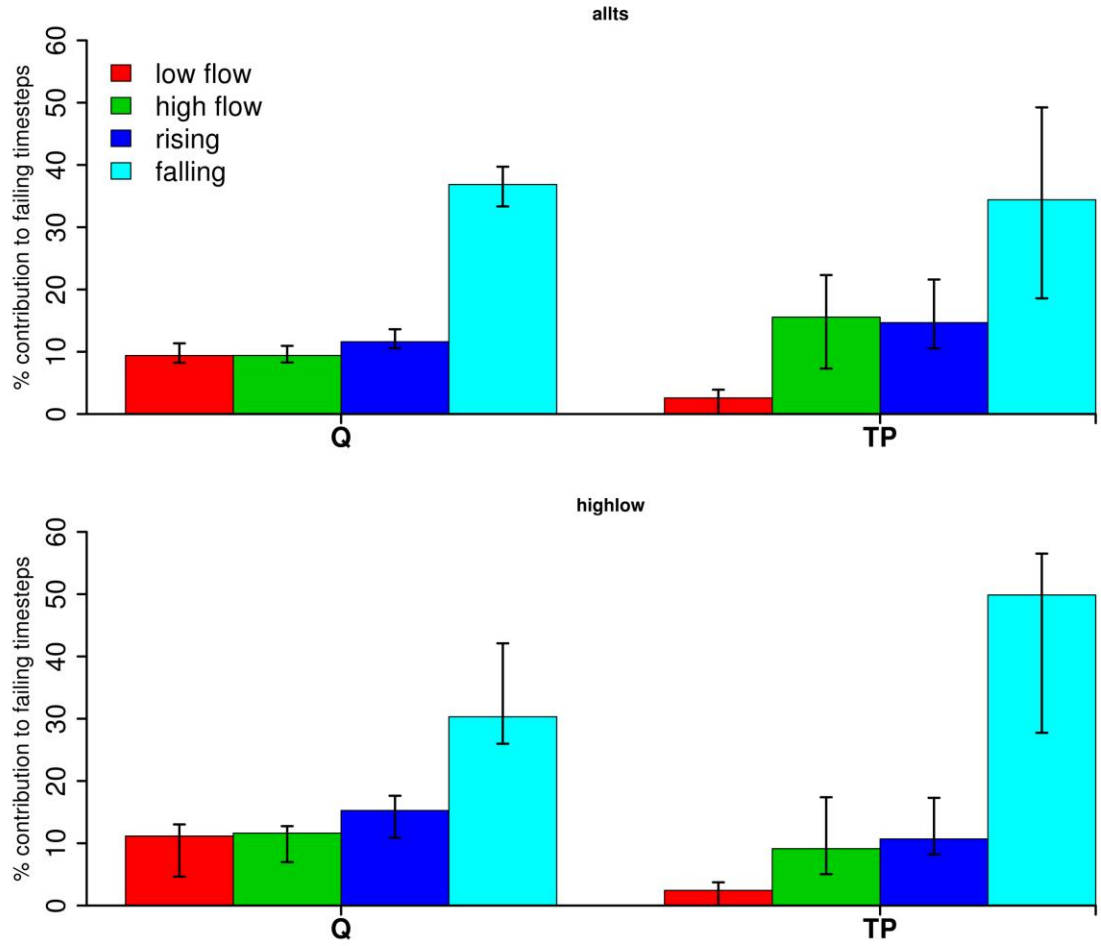

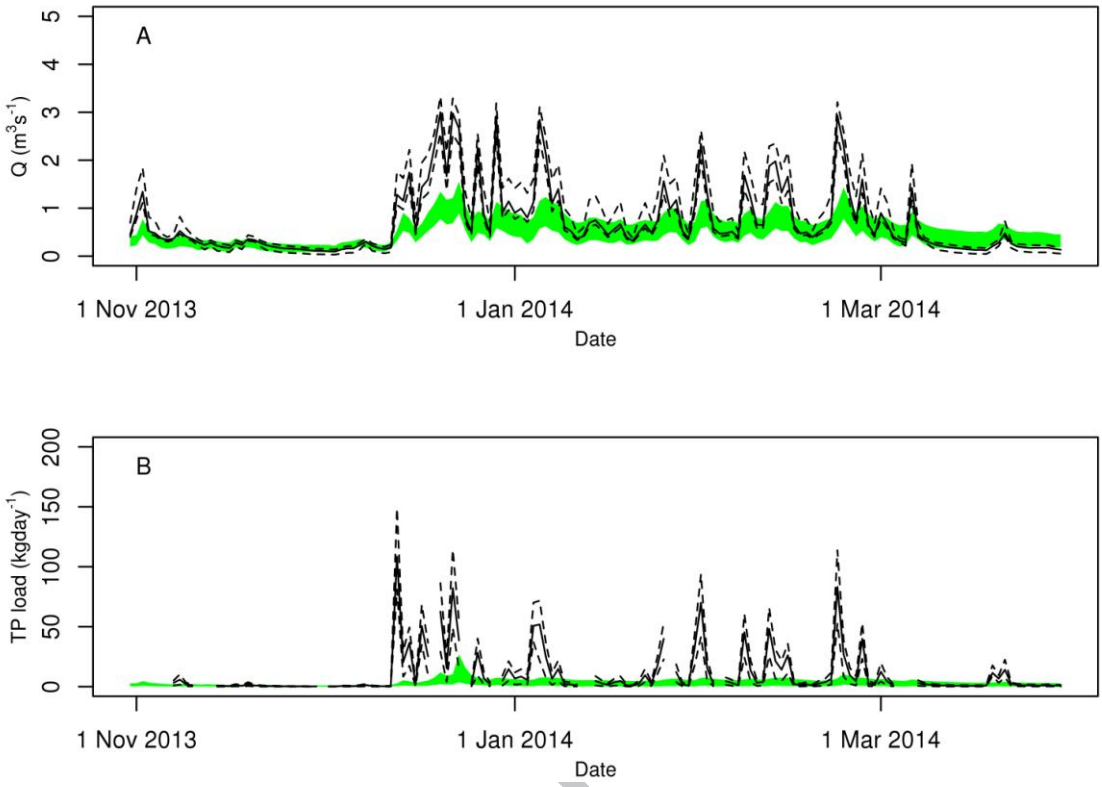

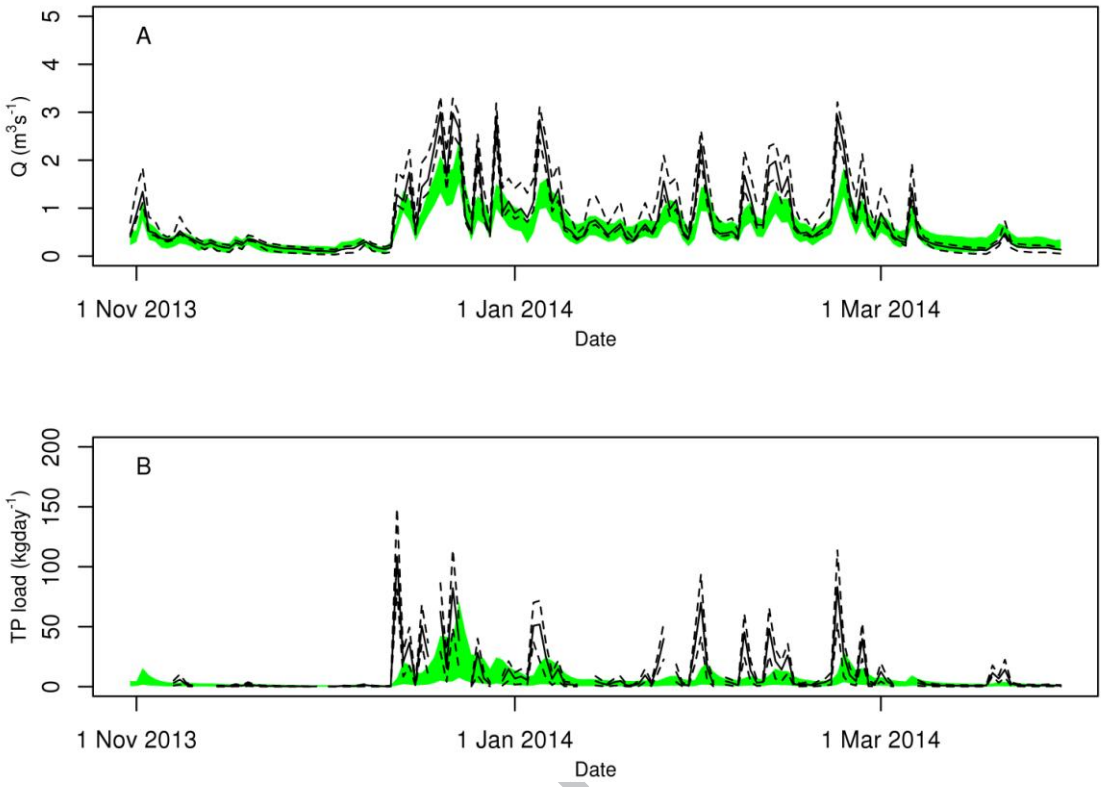

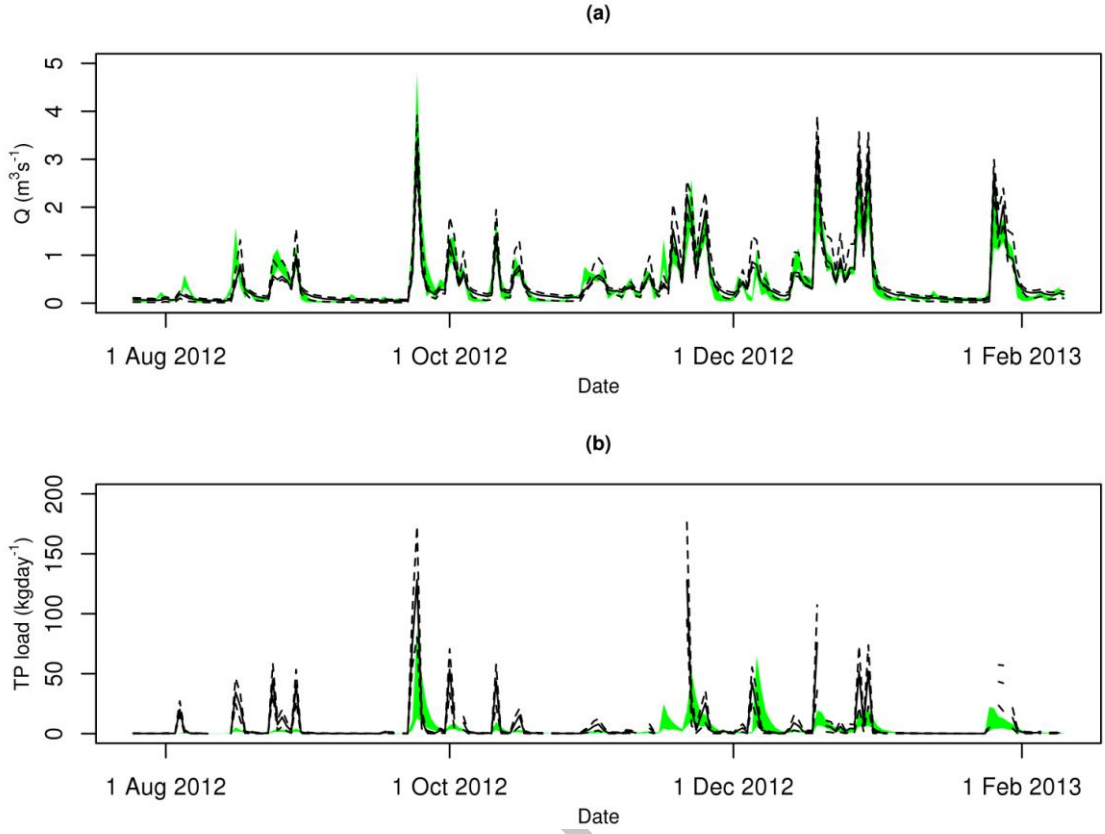

**Figure Captions**

**Figure 1: Summary of spatial data in the Newby Beck catchment. Panel a) shows the catchment topography, panel b) shows the locations of the monitoring station (discharge and total phosphorus (TP)), weather station and rain gauges, panel c) shows the main soil classes in the catchment and panel d) shows the broad land use classifications.**

**Figure 2: Generalised likelihood uncertainty estimation (GLUE) likelihood distributions, based upon the evaluation of models using criteria set for all time steps (normalized scores of ± 6.72), of Qsim (simulated discharge), normalised score for Q (discharge), TP loadsim (simulated total phosphorus) and normalised scores for TP, respectively, against observations (panels A-D). The plots are repeated for the low flow periods (panels E-H), rising time-steps (panels I-L), falling (recession) time-steps (panels M-P) and high flow periods (panels Q-T). The areas between the distribution percentiles max/min, $5^{th}$/$95^{th}$ and $25^{th}$/$75^{th}$ are shown in grey shades of increasing intensity. The medians of the distribution are shown by black dots. 1:1 lines and normalised scores of 0 lines have been added for orientation**

**Figure 3: Generalized Likelihood Uncertainty Estimation (GLUE) weighted prediction bounds (green shading) for discharge (a) and total phosphorus loads (b) for Newby Beck outlet (part of the calibration period) based on normalized scores on both discharge and total phosphorus (TP) load evaluation measures when criteria (normalized scores of ± 6.72) set over all model time-steps (1016 simulations). The black line in each plot shows the observed discharge (a) and TP loads (b), respectively. The dashed lines show the uncertainty limits on the calibration data.**

**Figure 4: Generalised Likelihood Uncertainty Estimation (GLUE) likelihood distributions of, based upon the evaluation of models using criteria set for high and low flow periods only (normalized scores of ± 5.30), Qsim (simulated discharge), normalised score for Q (discharge), TP loadsim (simulated total phosphorus) and normalised scores for TP, respectively, against observations (panels A-D). The plots are repeated for the low flow periods (panels E-H), rising time-steps (panels I-L), falling (recession) time-steps (panels M-P) and high flow periods (panels Q-T). The areas between the distribution percentiles max/min, $5^{th}$/$95^{th}$ and $25^{th}$/$75^{th}$ are shown in grey shades of increasing intensity. The medians of the distribution are shown by black dots. 1:1 lines and normalised scores of 0 lines have been added for orientation.**

**Figure 5: Generalized Likelihood Uncertainty Estimation (GLUE) weighted prediction bounds (green shading) for discharge (a) and total phosphorus loads (b) for Newby Beck outlet (part of the calibration period) based on normalized scores on both discharge and total phosphorus (TP) load evaluation measures when criteria (normalized scores of ± 5.30) set over high and low flow time-steps only (1001 simulations). The black line in each plot shows the observed discharge (a) and TP loads (b), respectively. The dashed lines show the uncertainty limits on the calibration data.**

**Figure 6: Dotty plots for 39 of the parameters varied in the Monte-Carlo runs. Parameter names and definitions are shown in Table 1. These are based on the 1016 behavioural simulations evaluated across all time-steps (normalized scores of ± 6.72).**

**Figure 7: Dotty plots for 39 of the parameters varied in the Monte-Carlo runs. Parameter names and definitions are shown in Table 1. These are based on the 1001 behavioural simulations evaluated across the high and low flow time-steps only (normalized scores of ± 5.30).**

**Figure 8: Breakdown of classification of time-steps resulting in model failure for the 1016 simulations constrained on all time-steps (upper panel) and the 1001 simulations constrained on the high and low flow periods only (lower panel). The bars show the median % contribution to failing time-steps and the error bars show the 2.5/97.5$^{th}$ percentiles from the Generalised Likelihood Uncertainty Estimation (GLUE) weighted distributions.**

**Figure 9: Generalized Likelihood Uncertainty Estimation (GLUE) weighted prediction bounds (green shading) for discharge (a) and total phosphorus (TP) loads (b) for Newby Beck outlet during the validation period (winter of the 2013-2014 Hydrological year) using the 1016 behavioural simulations accepted on both discharge and total phosphorus load criteria when evaluating constrained across all time-steps. The black line in each plot shows the observed discharge (a) and TP loads (b), respectively. The dashed lines show the uncertainty limits on the calibration data.**

**Figure 10: Generalized Likelihood Uncertainty Estimation (GLUE) weighted prediction bounds (green shading) for discharge (a) and total phosphorus (TP) loads (b) for Newby Beck outlet during the validation period (winter of the 2013-2014 Hydrological year) using the 1001 behavioural simulations accepted on both discharge and total phosphorus load criteria when evaluating constrained across high and low flow time-steps only. The black line in each plot shows the observed discharge (a) and TP loads (b), respectively.**

**Figure 11: Generalized Likelihood Uncertainty Estimation (GLUE) weighted prediction bounds (green shading) for discharge (a) and total phosphorus loads (b) for Newby Beck outlet (part of the calibration period) based on normalized scores on both discharge and total phosphorus (TP) load evaluation measures when criteria set over 95% of time steps (1057 simulations). The black line in each plot shows the observed discharge (a) and TP loads (b), respectively.**

**Highlights**

This limits of acceptability approach is applied for the first time to the SWAT model

Identifies exact time steps of poor performance during calibration

Accounts for evaluation data uncertainty in calibration

It may be difficult to obtain sufficient data to drive complex models with confidence